FLUID TRANSPORT IN THE RABBIT GALLBLADDER

A Combined Physiological and Electron Microscopic Study

GORDON I. KAYE, HENRY O. WHEELER, ROBERT T. WHITLOCK, and NATHAN LANE

From the F. Higginson Cabot Laboratory of Electron Microscopy of the Division of Surgical Pathology, Departments of Surgery and Pathology; and the Department of Medicine, College of Physicians and Surgeons of Columbia University, New York

ABSTRACT

The fine structure of the rabbit gallbladder has been studied in specimens whose functional state was undetermined, which were fixed either in situ or directly after removal from the animal; in specimens whose rate of fluid absorption was determined, either in vivo or in vitro, immediately prior to fixation; and in specimens from bladders whose absorptive function was experimentally altered in vitro. Considerable variation was found in the width of the epithelial intercellular spaces in the bladders whose functional state was undefined. In bladders known to be transporting fluid, either in vivo or in vitro, the intercellular spaces were always distended, as were the subepithelial capillaries. This distension was greatest in bladders which had been functioning in vitro. When either Na^+ or Cl^- was omitted from the bathing media, there was no fluid transport across the wall of the gallbladder studied in vitro. The epithelial intercellular spaces of biopsies taken from several bladders under these conditions were of approximately 200 A width except for minor distension at the crests of mucosal folds. The addition of the missing ion rapidly led to the reestablishment of fluid transport and the distension of the intercellular spaces throughout most of the epithelium of these bladders. Studies of sodium localization (by fixation with a pyroantimonate-OsO_4 mixture) showed high concentrations of this ion in the distended intercellular spaces. Histochemical studies of ATPase activity showed that this enzyme was localized along the lateral plasma membrane of the epithelial cells. The analogy is drawn between the structure of the gallbladder mucosa and a serial membrane model proposed by Curran to account for coupled solute-solvent transport across epithelia. It is concluded that the intercellular compartment fulfills the conditions for the middle compartment of the Curran model and that active transport of solute across the lateral plasma membrane into the intercellular space may be responsible for fluid absorption by the gall bladder.

INTRODUCTION

Studies of solute and water transport in the fish gallbladder (1–3) and rabbit gallbladder (4–8) have demonstrated that active, electrically neutral transport of sodium chloride creates the driving

force for the absorption of water from the gallbladder lumen, and that water absorption may even proceed against significant osmotic gradients.

In previous electron microscope studies of gallbladders in the mouse (9, 10), dog (11), and man (12), the tissues were fixed without knowledge of the absorptive state of the organs. We have undertaken to examine the fine structure of the rabbit gallbladder in experiments in which the rate of water absorption was measured immediately prior to fixation. From these studies, it has been possible to make correlations between the functional state and certain structural alterations in the mucosa. The significance of these correlations has been discussed in relation to recent theoretical suggestions regarding the mechanism of water absorption.

MATERIALS AND METHODS

Twenty-six gallbladders from New Zealand white rabbits were studied under various conditions.

Gallbladders of Undefined Functional State

Four gallbladders were fixed either in situ after Nembutal anesthesia by intraluminal injection of 1% OsO_4 in M/15 Sorensen's phosphate buffer (pH 7.4) or by mincing the bladder into the same fixative immediately after its removal from animals sacrificed by a blow on the head. Two other gallbladders were fixed in situ by intraluminal injection of a solution of 1% OsO_4 and 2% $KSb(OH)_6$ in 0.01 N acetate buffer (pH 7.8) to permit localization of regions of high sodium concentration as described by Komnick (13).

For histochemical demonstration of adenosinetriphosphatase activity, 4 gallbladders were fixed in 1 to 6% glutaraldehyde in 0.1 M cacodylate buffer (pH 7.0). Tissue was then reacted according to the procedure of Wachstein and Meisel (14) and postfixed in cold 1 to 2% OsO_4 in Veronal-acetate buffer (pH 7.4).

These 10 bladders constitute a random sampling of gallbladders of undefined functional state.

Gallbladders Functioning in Vivo

Two gallbladders were exposed surgically during Nembutal anesthesia and a fine polyethylene tube was tied into the cystic duct without disturbing the blood supply (8). The contents of the gallbladder were aspirated, using a graduated syringe, and replaced in one case with 0.92 ml of the freshly aspirated bile and in the other case with 1.0 ml of a solution of 20% ThO_2 in Krebs-Henseleit bicarbonate buffer (15). After 1 hr, the residual luminal volume of these bladders was measured (in order to calculate the rate of water absorption), a solution of 1% OsO_4 in Sorensen's phosphate buffer (pH 7.4) was injected into the lumen, and the bladders were removed immediately for mincing and further fixation.

Gallbladders Studied in Vitro

The remaining 14 gallbladders were removed from rabbits sacrificed by a blow on the head and studied in vitro at 37° in a chamber which has been described previously (5). In this apparatus, the gallbladder was mounted as a sac on the end of a glass cannula, and the mucosal and serosal bathing media were circulated continuously by a stream of 5% CO_2–95% O_2 gas mixture. In addition to the composition noted below, the bathing media in all in vitro experiments contained glucose (1 mg/ml). The rate of water transport through the bladder wall was estimated by serial measurements of the volume of the serosal bath.

Gallbladders Bathed in Isotonic Krebs-Henseleit Solution

Five gallbladders bathed in Krebs-Henseleit bicarbonate solution (15) whose rate of water absorption was measured for approximately 1 hr were fixed by cutting the gallbladder from its cannula into a pool of cold 1% OsO_4 in Sorensen's phosphate buffer (pH 7.4). In 2 of these experiments the mucosal fluid contained approximately 4% ThO_2.

Experimentally Altered Gallbladder Function in Vitro

In addition to the above experiments, gallbladders were studied in bathing fluids which were modified in various ways to alter or inhibit normal solute and solvent transport across the wall.

Osmotic Inhibition of Solvent Flux

In 1 experiment, Krebs-Henseleit bicarbonate solution (15) was placed in both the mucosal and serosal baths, but the mucosal fluid was made hyperosmotic by the addition of sucrose to a concentration of 0.115 M to inhibit water flux while NaCl flux continued. The rate of net sodium transport through the gallbladder wall was estimated by serial measurements of the sodium concentration in samples of the mucosal bath (5) in a Baird model DB-4 flame spectrophotometer.

Inhibition of Transport by Ionic Substitution

In 6 experiments, gallbladders were bathed in Na-free mucosal and serosal solutions containing tetraethylammonium chloride (TEACl) and tetraethylammonium bicarbonate ($TEAHCO_3$) in place

of NaCl and $NaHCO_3$ in the Krebs-Henseleit solution. After approximately 40 min (in one case 85 min) in the Na-free solution, the sodium concentration in the mucosal bath was raised from zero to approximately 30 mEq/l by partial substitution of a solution of NaCl and $NaHCO_3$ for the Na-free solution.

Specimens of tissue were taken at various times during the course of the studies by lifting the bladder from the chamber, ligating the fundic end, and carefully cutting off this end so that it fell directly into a vial of cold fixative. Such specimens will be referred to throughout these studies as "biopsies." The procedure allowed us to sample a small portion of the gallbladder during a specific experimental condition and to return the major portion of the bladder to the chamber for further study.

One bladder was biopsied twice (at 15 and 85 min) before the addition of sodium, while 2 bladders were biopsied 1 and 2 min, respectively, after the addition of sodium to the mucosal bath. In the other 3 bladders a single biopsy was obtained immediately before addition of sodium to the lumen.

Thirty to 60 min after addition of sodium to the mucosal fluid, the gallbladders were removed from the chamber, cut from the cannula into a pool of the Na-free solution, and divided longitudinally. One-half was fixed in 1% OsO_4 in Sorensen's phosphate buffer (pH 7.4) and one-half was fixed in the solution described by Komnick (13) which contained 2% potassium pyroantimonate ($KSb(OH)_6$) and 1% OsO_4 in 0.01 N acetate buffer (pH 7.8). Two of the biopsies were fixed in the former solution and the other 4 were fixed in the latter.

In 2 experiments, a chloride-free solution was employed which was similar to Krebs-Henseleit bicarbonate solution except that sulfate instead of chloride was the major anion and sodium concentration was 185 instead of 143 mEq/l. In 1 of these 2 experiments, the gallbladder was first bathed in Krebs-Henseleit solution. After a short period during which it was determined that the bladder was functioning, the serosal fluid was changed to the solution described above and the mucosal bath was filled with a 0.104 M solution of Na_2SO_4. Both solutions had an osmolality of 260 milliosmols/Kg. After 50 min under these conditions, one-fifth of the fluid in the mucosal bath was removed and replaced with an equal volume of a solution containing Na, 154 mEq/l; Cl, 129 mEq/l; and HCO_3, 25 mEq/l. A biopsy was taken just prior to this change and the remaining portion of the bladder was fixed 50 min later in 1% OsO_4 in Sorensen's phosphate buffer.

In the other experiment, the bladder was initially bathed in the Cl-free solution described above and the mucosal bath filled with 0.104 M Na_2SO_4. After 30 min, the fundic dome was biopsied and one-fifth of the mucosal fluid was removed and replaced with the NaCl-$NaHCO_3$ solution described above. After an additional 90 min, the remaining portion of the bladder was removed from the chamber and fixed.

Fixation and Embedding

After initial fixation, all bladders were divided into fundic, mid, and cystic portions which were separately minced in cold fixative, fixed for 1 to 2 hr, dehydrated in a graded series of ethanol solutions, and embedded in Epon 812 (16).

Precise orientation of the mucosa was achieved by the following procedure:

Tissue was cut into strips of approximately 1×3 mm. When the tissue was in the final resin mixture prior to embedding, a No. 15 minutin pin was inserted a short distance into one end of the strip. The other end of the pin was passed through a 6-mm diameter disc punched from an index card. This assembly was lowered into a gelatin or polyethylene capsule prefilled with resin. The disc of index card floated on the top of the resin and the tissue could be oriented in the proper direction and centered near the bottom of the capsule by moving the pin.

Orientation was confirmed by examining 1- to 2-μ sections of tissue blocks by phase contrast microscopy. Thin sections were cut on a Porter-Blum MT-1 or Huxley microtome using glass or diamond knives, stained with uranyl acetate and lead citrate (17), carbon coated, and examined in an RCA EMU-3G.

RESULTS

Gallbladders of Undefined Functional State

The histology of the rabbit gallbladder is essentially that described for the human gallbladder in standard textbooks of histology or pathology (18, 19). The gallbladder is lined with a single layer of tall columnar epithelial cells. The major folds of the gallbladder mucosa form crests and valleys with groups of epithelial cells forming cobblelike structures along the lateral surfaces of the major folds (Fig. 1). The epithelial cells at the crests of the folds are taller than those in the depths of the valleys, and those in the center of the epithelial cobbles are taller than those in the periphery of the cobbles. In addition, minor folds are sometimes found projecting into the lumen near the bases of major folds. These are short and thin, and their surface is smooth, rather than cobbled.

Electron microscope examination of 10 rabbit gallbladders revealed an epithelial fine structure closely resembling that in the mouse (9, 10), dog (11), and human (12). Small microvilli capped with *antennulae microvillares* covered the apical (luminal) surface of the epithelial cells (Fig. 2).

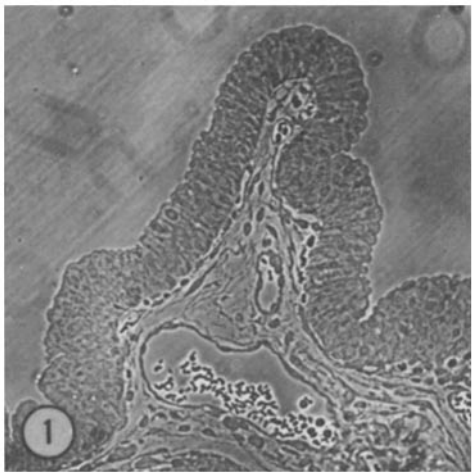

FIGURE 1 This low power phase contrast micrograph shows the tip of a mucosal fold of the rabbit gallbladder. Variations in the height of the epithelial cells produce the cobbles seen at the right and left margins. Note the close proximity of the blood vessels to the base of the epithelium. × 175.

Invaginations of the plasma membrane were found in the intermicrovillous spaces. Numerous small vesicles in the clear apical cytoplasm were lined with hairlike projections resembling those of the microvilli and intermicrovillous spaces of the luminal surface, suggesting that some pinocytosis can occur at this surface (Fig. 2). A typical apical junctional complex (20) sealed the luminal end of the epithelial intercellular space. The intercellular space was relatively straight as it passed the apical mitochondrial zone. Complex lateral interdigitations and plications of the lateral plasma membrane began at the nuclear level (Fig. 3) and increased in number and complexity towards the basal lamina (Fig. 4). Desmosomes were rare along the long columnar segment of the cell, but occurred near the basal end in some areas of the epithelium (Fig. 4).

The size of the epithelial intercellular spaces and the morphology of the subepithelial capillaries varied considerably both within single gallbladders and among all 10 gallbladders studied, even though these bladders were treated identically.

In 4 of the 10 gallbladders, the entire epithelial intercellular space was of the 150- to 200-A width previously thought to be typical of most epithelia. In these bladders, collapsed capillaries with thick endothelia were found closely applied to the basal surface of the epithelium (Fig. 5).

In the other 6 gallbladders, the epithelial intercellular spaces were distended at their basal ends to varying degrees up to approximately 2 μ. Distension of the intercellular spaces was most commonly found near and at the tips of the mucosal folds in the fundic and mid portions of the gallbladders (Fig. 6). Although distension of the spaces was sometimes observed along the upper half of the sides of the folds, especially in the center of the epithelial cobbles, no distension was ever found in the depths of the valleys. Whenever the spaces were distended, the subepithelial capillaries were also distended and had attenuated, fenestrated endothelia (Fig. 6). The capillaries near the tips of the folds in which these morphological variations commonly occurred were separated from the basal lamina of the epithelium by a thin, clear zone of lamina propria, with only occasional fibroblast processes seen between the two basal laminae; at the depths of the valleys, a fibroblast or fibroblast process formed a continuous layer between the epithelium and the subjacent capillary.

The 2 gallbladders fixed in the pyroantimonate-osmium mixture ($KSb(OH)_6$–OsO_4) showed only moderate distension of the intercellular spaces at or near the crests of the mucosal folds. All other areas of the epithelium had intercellular spaces of approximately 200-A width. There were large particles of sodium pyroantimonate in the distended spaces (Fig. 7). Precipitate was also found in the immediately subjacent lamina propria and subepithelial blood vessels in areas of distended epithelial intercellular spaces (Fig. 8). In some areas in which the spaces were not distended, particularly in the upper half of the mucosal folds, $NaSb(OH)_6$ appeared to be localized along the intracellular side of the plasma membrane. In the lower half of the mucosal folds and in the cells at the depths of the valleys, where no distenstion of the intercellular spaces was ever seen, a light nonspecific dusting of precipitate was found over the cytoplasm.

In the 4 gallbladders reacted for ATPase activity, the lead phosphate end product was localized on the extracellular side of the lateral plasma membrane and in the intercellular space, particularly in the apical (Fig. 9) and nuclear (Fig. 10) zones. In these figures, it is clear that the pattern of lead phosphate distribution exactly follows the

FIGURE 2 A portion of the apical end of two gallbladder epithelial cells. Microvilli covered with hairlike projections are seen at the luminal surface. Invaginations of the plasma membrane in the intermicrovillous spaces and vesicles (*V*) lined on the inside with hairlike material, apparently identical to that seen on the microvilli, suggest that pinocytosis may occur at this surface. A typical junctional complex (*J*) is seen at the apical end of the intercellular space. *M*, mitochondria. × 30,000.

FIGURE 3 Complex lateral plications between two epithelial cells at the nuclear level. × 30,000.

complex convolutions of the intercellular space. In our preparations, the apical and basal plasma membranes had no lead phosphate end product associated with them.

Previous reports on other species (9–12), which dealt with small samples of gallbladder epithelium from unspecified zones of the mucosa, described distension of the intercellular space as a regular finding and suggested that this might be related to the absorptive function of the gallbladder. The variability which we found in the cytology of the mucosa of different bladders suggested differences in functional state of the bladders at the time of fixation. Therefore, bladders were studied in controlled functional states in an attempt to determine the significance of the variable morphology of the mucosa of normal bladders.

Gallbladders Functioning in Vivo

In the gallbladder dehydrating its bile at a rate of 550 μl/hr, the epithelial intercellular spaces were distended (Fig. 11). The spaces maintained a width of approximately 200 A in the supranuclear region of the epithelium, were minimally distended in the nuclear region, and reached greatest width in the basal region (Fig. 11). It could be seen here, however, as in the 10 gallbladders described above (Figs. 6 and 7), that the intercellular space immediately above the basal lamina was always maintained at approximately 200 to 500 A by the extension of the basal processes of the epithelial cells along the basal lamina. Each intercellular space in longitudinal section had the silhouette of a pine tree, with the intercellular space gradually widening from 200 A at the nuclear level to as much as 2 to 3 μ near the base, but abruptly returning to 200 to 500 A at the opening onto the basal lamina. However, it should be noted that the spaces are continuously connected and form a single labyrinthine compartment surrounding all of the epithelial cells.

In the gallbladder functioning in vivo with Krebs-Henseleit solution substituted for its bile (absorbing water from the lumen at a rate of 960 μl/hr), the distension of the intercellular space was much greater (Fig. 12) than in the gallbladder dehydrating its own bile (Fig. 11). As always, however, the basal processes extended along the basal lamina so that the 200- to 500-A width of the intercellular space was maintained at that point. In a cross-section at the nuclear level of the epithelium of this gallbladder (Fig. 13) it was seen that the separation of the cells was greatest at the points at which three or more cells would usually abut. The subepithelial capillaries in these gallbladders functioning in vivo were distended and had greatly attenuated, fenestrated endothelia (Fig. 12). These capillary changes were limited, however, to the zones of the mucosa in which the epithelial intercellular spaces were distended. At the depths of the valleys, where the epithelial intercellular spaces were not distended, the subepithelial capillaries were collapsed or minimally distended.

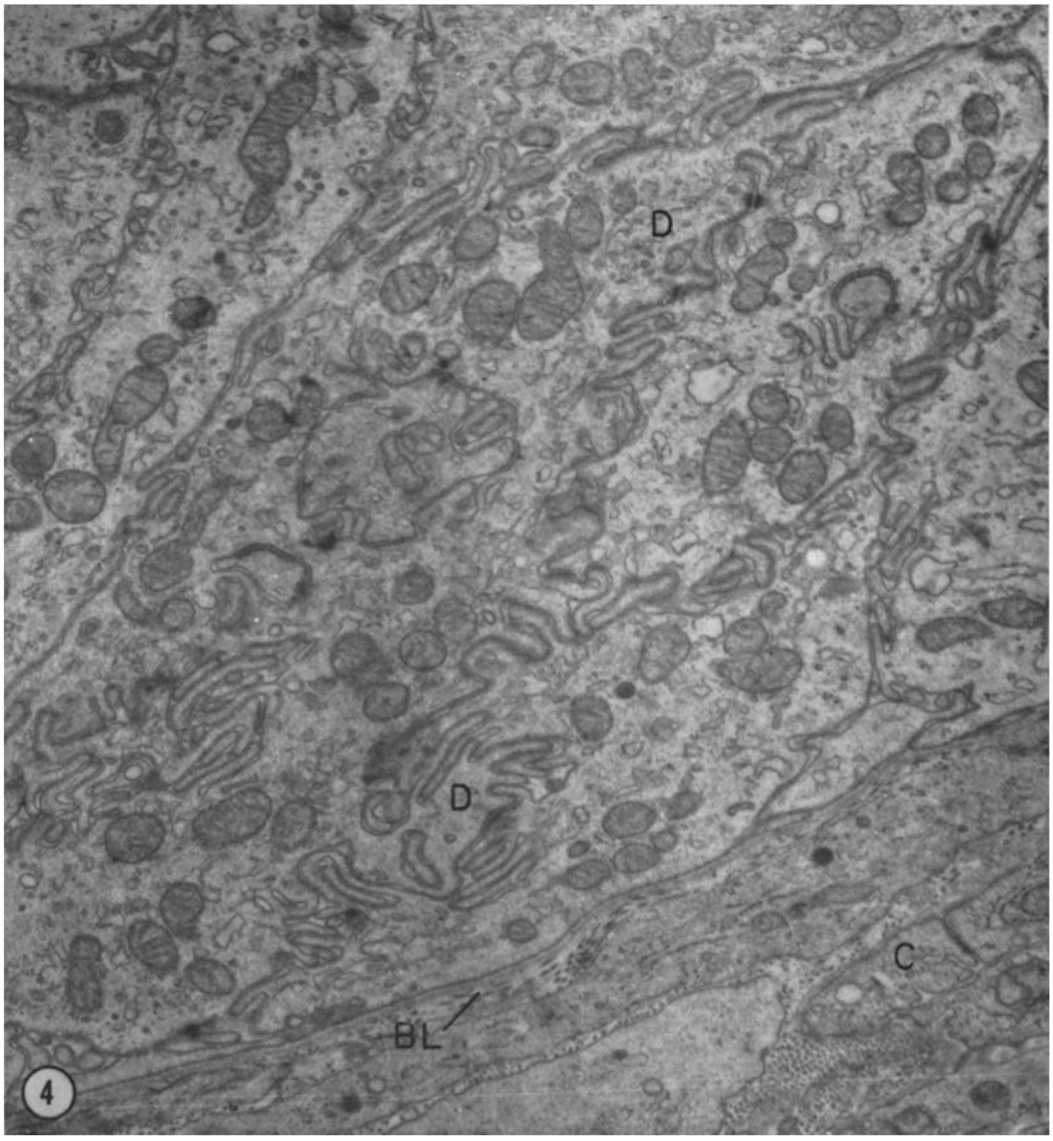

FIGURE 4 Low power electron micrograph of the basal ends of several epithelial cells showing the extremely complex lateral plications of adjacent cells at this level. A few desmosomes (*D*) are seen between the cells but there are no specialized structures, such as half desmosomes, between the bases of the cells and the underlying basal lamina (*BL*). A collapsed capillary (*C*) is seen in the lamina propria. × 16,000.

There was some uptake of ThO_2 by pinocytosis. A few pinocytotic vesicles containing ThO_2 were found in the apical cytoplasm, and small vacuoles containing ThO_2 were found in the nuclear region of the epithelial cells of this gallbladder (Fig. 13). There was no evidence, however, either in vivo or in vitro, for the transport of ThO_2 particles out of the cell across the lateral or basal plasma membrane.

Gallbladders Studied in Vitro

GALLBLADDERS BATHED IN ISOTONIC KREBS-HENSELEIT SOLUTION

Of the 5 gallbladders bathed in Krebs-Henseleit solution, 4 transported solution rapidly from the lumen to the serosal bath, at rates ranging from 193 to 465 μl/hr. All of the 4 showed the

same morphology when fixed after approximately 1 hr of function in vitro. The epithelial intercellular spaces were dilated to a considerably greater degree than in the in vivo studies described above. In these in vitro studies, the distension of the intercellular spaces was seen at all levels of the mucosal folds, with the usual exception of the depths of the valleys. The crests of the folds and the centers of the cobbles showed the largest intercellular spaces.

The extreme degree to which the intercellular spaces can expand is well shown in a low power electron micrograph (Fig. 14). In specimens from the in vitro studies, the space was distended almost up to the region of the apical junctional complex (Figs. 14 and 15). The epithelial cells appeared as columns surrounded by a fluid compartment (Fig. 16). The lateral processes (Fig. 16) were those which formed the lateral interdigitations and plications between the epithelial cells (Figs. 3 and 4). Even with this extreme distension, the apical junctional complex, however, remained intact (Fig. 15); the basal surface of the epithelial cells also always remained firmly attached to the basal lamina; and the width of the intercellular space at the level of the basal lamina was maintained at 200 to 500 A by the close apposition of basal processes (Fig. 17).

The fifth gallbladder bathed in Krebs-Henseleit solution exhibited no measurable absorptive activity despite the fact that it appeared grossly normal and was excised and mounted without technical difficulty. The absence of transport could not be attributed to abnormalities in the apparatus or bathing media since another bladder, mounted immediately thereafter and bathed in the same solutions, exhibited vigorous fluid absorption (234 μl/hr). The nonfunctioning bladder was removed and fixed after 53 min of observation. Examination of this tissue with the phase and electron microscopes showed that there were several traumatized areas of epithelium in which the epithelial cells were detached from the basal lamina. There was also considerable edema of the lamina propria. The epithelial cells in the nontraumatized areas of the mucosa appeared identical with those of the 4 other bladders studied in vitro.

Experimentally Altered Gallbladder Function in Vitro

Osmotic Inhibition of Solvent Flux

With a hypertonic solution in the gallbladder lumen, active transport of sodium continued at the rate of 80 μEq/hr, but water flux was reduced to less than 15 μl/hr. This bladder did not show the consistent cytological pattern observed in the 4 bladders (above) functioning in isotonic media. Instead, while some areas of the mucosa showed moderate or extreme distension of the epithelial intercellular space at and near the tips of the mucosal folds, other areas showed no distension in comparable locations (Figs. 18 and 19).

Inhibition of Transport by Ionic Substitution

The total substitution of tetraethylammonium ion for sodium ion in the bathing solutions completely arrested water transport across the wall of the gallbladder (Fig. 20). The addition of Na to the solution bathing the mucosal surface led, after 15 to 30 min, to vigorous transport of NaCl and water across the wall of the gallbladder (Fig. 20). Rates of water flux ranged from 90 to 320 μl/hr in the 6 bladders studied. Continuous recording of the electrical potential difference across the gallbladder wall suggested that transport of NaCl actually was reestablished within 3 min after the addition of Na to the mucosal bath (Fig. 21), and the lag in detection of transmural water flux could

FIGURE 5 Basal end of two epithelial cells from a gallbladder in which the epithelial intercellular spaces were of 150- to 200-A width. A collapsed capillary (*C*) is in close proximity to the basal lamina of the epithelium. × 16,000.

FIGURE 6 An area similar to that shown in Fig. 5 from a gallbladder with distended epithelial intercellular spaces (*IC*). A distended capillary (*C*) with an attenuated fenestrated endothelium is found beneath the epithelium. Note the absence of a continuous layer of cellular processes between the basal lamina (*BL*) of the epithelium and that of the endothelium. × 16,000.

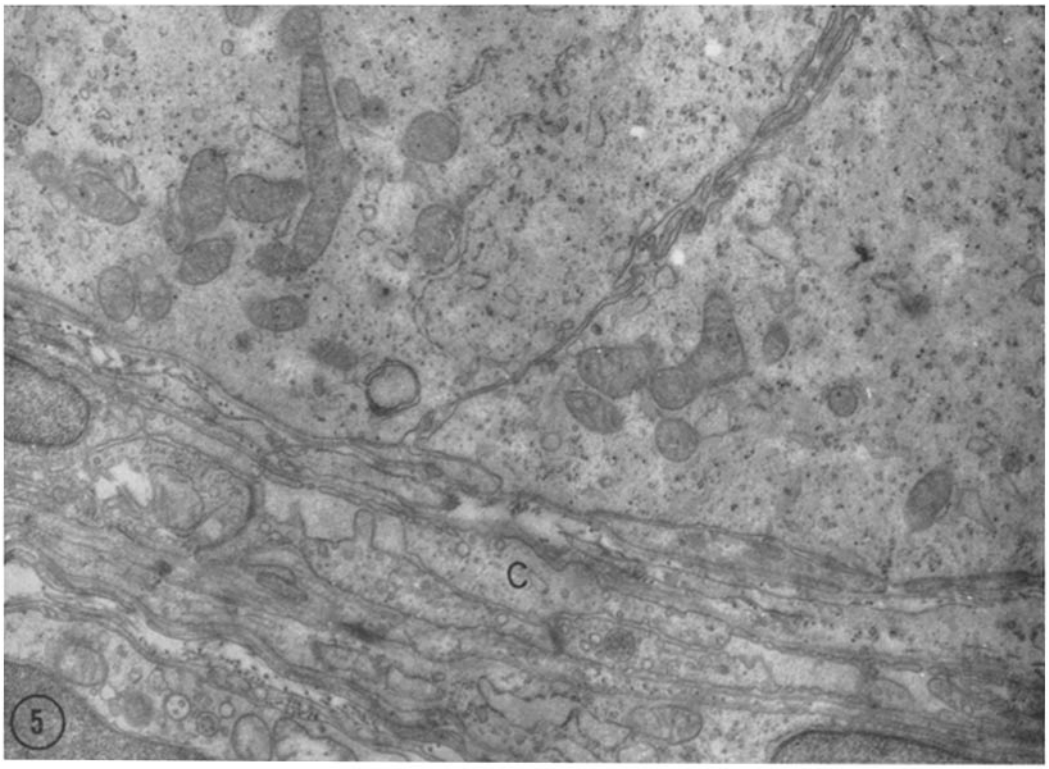
C
5

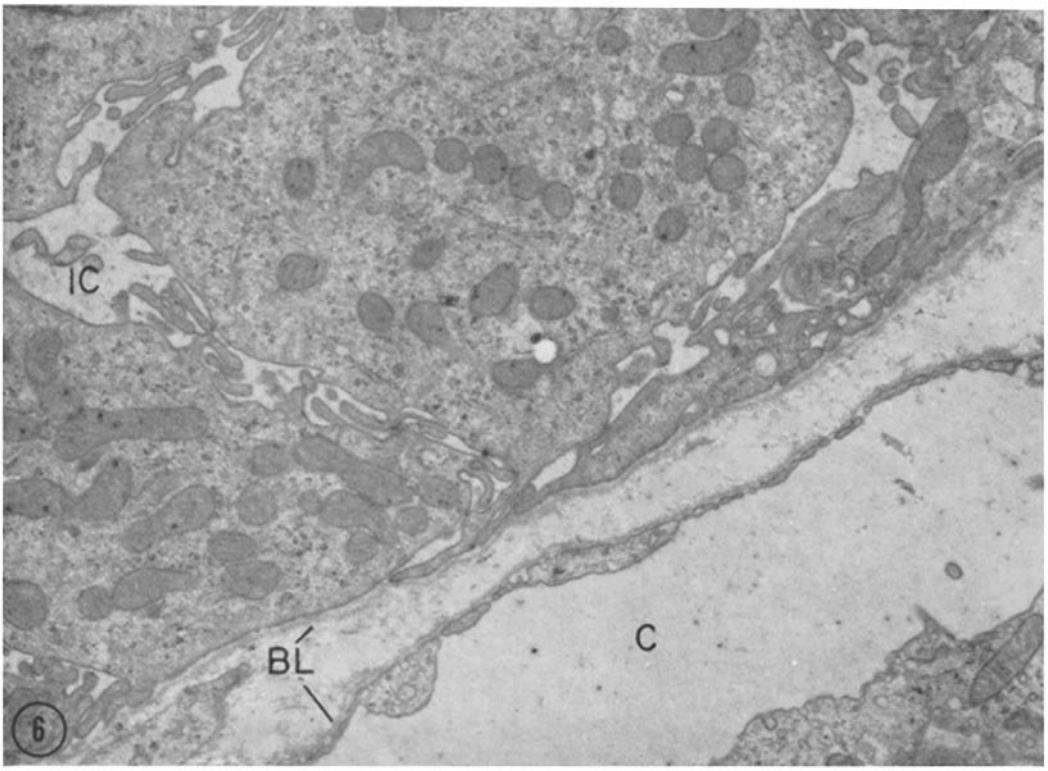
IC
BL
C
6

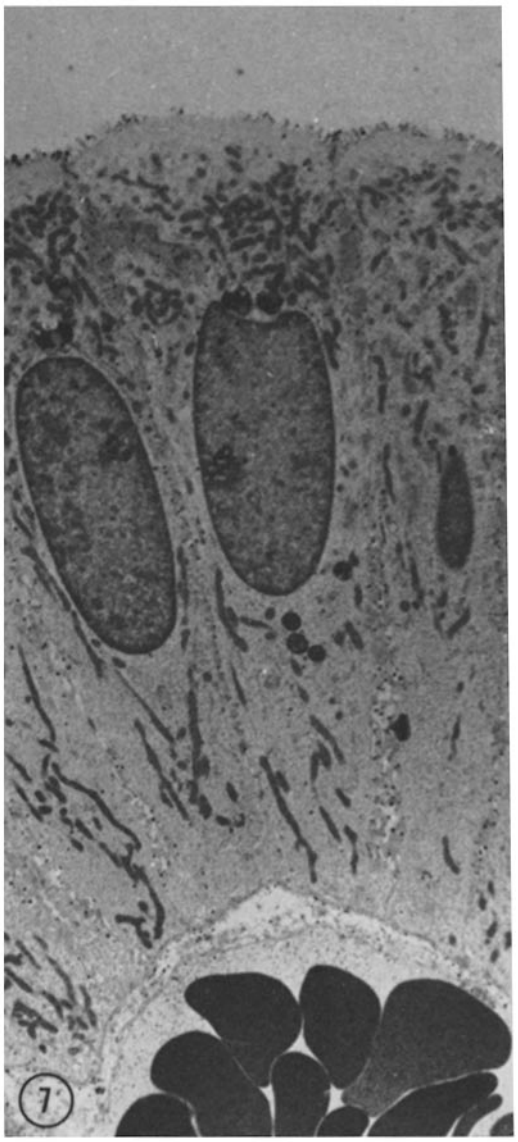

FIGURE 7 Low power electron micrograph of a gallbladder of undetermined functional state fixed in the pyroantimonate-OsO_4 mixture. The intercellular spaces are minimally distended, even at the crest of the mucosal fold. Precipitate of $NaSb(OH)_6$ is found in the intercellular spaces. × 2,800.

probably be attributed to initial accumulation of transported fluid in the bladder wall.

Using the biopsy technique, it was possible to obtain tissue from bladders in the nonfunctioning state for comparison with tissue obtained from the same bladders after initiation of active fluid absorption.

Biopsies of the fundus of gallbladders bathed in Na-free solution showed no distension of the epithelial intercellular spaces along the sides of the mucosal folds and only moderate distension at the extreme crests of the folds (Figs. 22 and 23), which is probably a residue of function prior to bathing in Na-free solution. The remaining portions of the same bladders, fixed after the addition of sodium to the mucosal bathing medium, showed marked distention of the intercellular spaces. In the biopsies obtained 1 and 2 min after the addition of sodium, distension was already apparent at the crests of the mucosal folds; and, in all specimens fixed 30 to 60 min after sodium addition, distended spaces were found along the entire length of each fold (Figs. 24 and 25). In other words, the intercellular spaces of a gallbladder in the nonfunctioning state were of approximately 200 A width, while those of the same bladder in the functioning state showed the same pattern and degree of intercellular distension seen in the 5 bladders which were bathed in Krebs-Henseleit solution from the outset.

In the gallbladder biopsied at both 15 and 85 min in Na-free media (with net water flux of zero), the epithelial intercellular spaces, except at the extreme crests of mucosal folds, were of approximately 200-A width at both time points (Fig. 26 *a* and *b*). Again, however, the remainder of the bladder, fixed approximately 60 min after the addition of sodium to the mucosal bath (net water flux 270 μl/hr), showed extensive and extreme distension of the epithelial intercellular spaces (Fig. 27). In all of these experiments, however, distension of spaces was never found at the depths of the valleys.

Substitution of sulfate for chloride similarly inhibited solute and water transport. The 2 gallbladders from the SO_4 substitution studies also showed intercellular spaces of approximately 200 A width in the nonworking state (Fig. 28) and distended intercellular spaces in the same gallbladders after addition of NaCl-$NaHCO_3$ solution to the lumen had resulted in net rates of water flux of 90 and 160 μl/hr (Fig. 29).

OBSERVATIONS ON SODIUM LOCALIZATION

Specimens of 5 gallbladders, fixed in the pyroantimonate-OsO_4 mixture after active fluid absorption had been initiated by addition of sodium

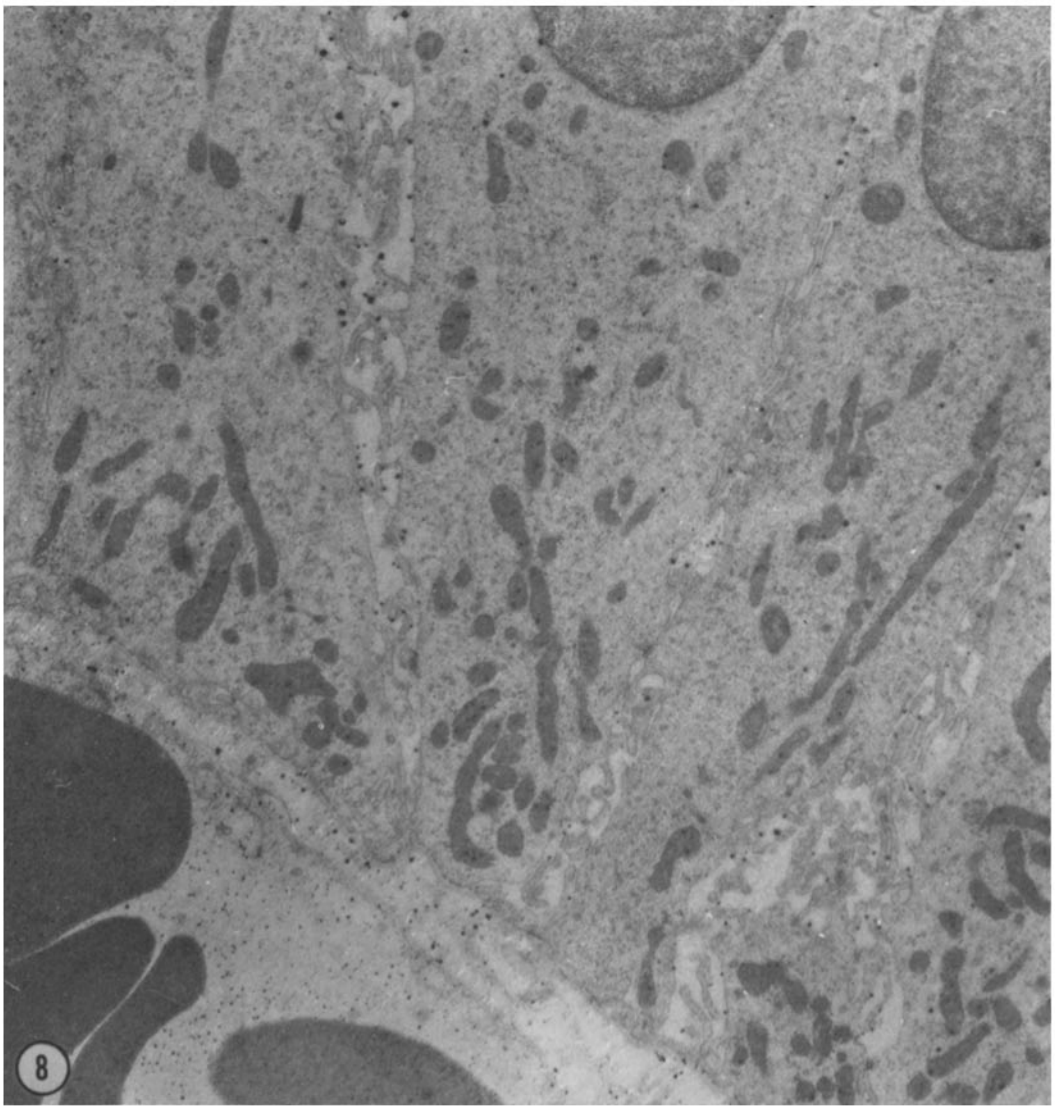

FIGURE 8 Higher magnification view of the bases of several epithelial cells from the same crest shown in Fig. 7. Precipitate of $NaSb(OH)_6$ is found primarily in the distended spaces as well as in the lamina propria and the underlying capillary. There is some precipitate of small particles in the cytoplasm. × 10,000.

to the lumen, showed a distribution of precipitate of sodium pyroantimonate identical with that described above for bladders fixed in the same solution in situ (Fig. 8). There were large particles of precipitate in the distended intercellular spaces (Fig. 30) and small particles in the cytoplasm. There was some preferential localization of precipitate along the intracellular side of the lateral plasma membrane at the supranuclear level of the epithelium (Fig. 31) in some areas in which the intercellular spaces were not distended. Large particles of precipitate of $NaSb(OH)_6$ could be found in the distended intercellular spaces as early as 1 and 2 min after the addition of sodium to the lumen. There was a large amount of precipitate in the lamina propria in areas in which the epithelial intercellular spaces were distended.

A biopsy from 1 gallbladder, which had been

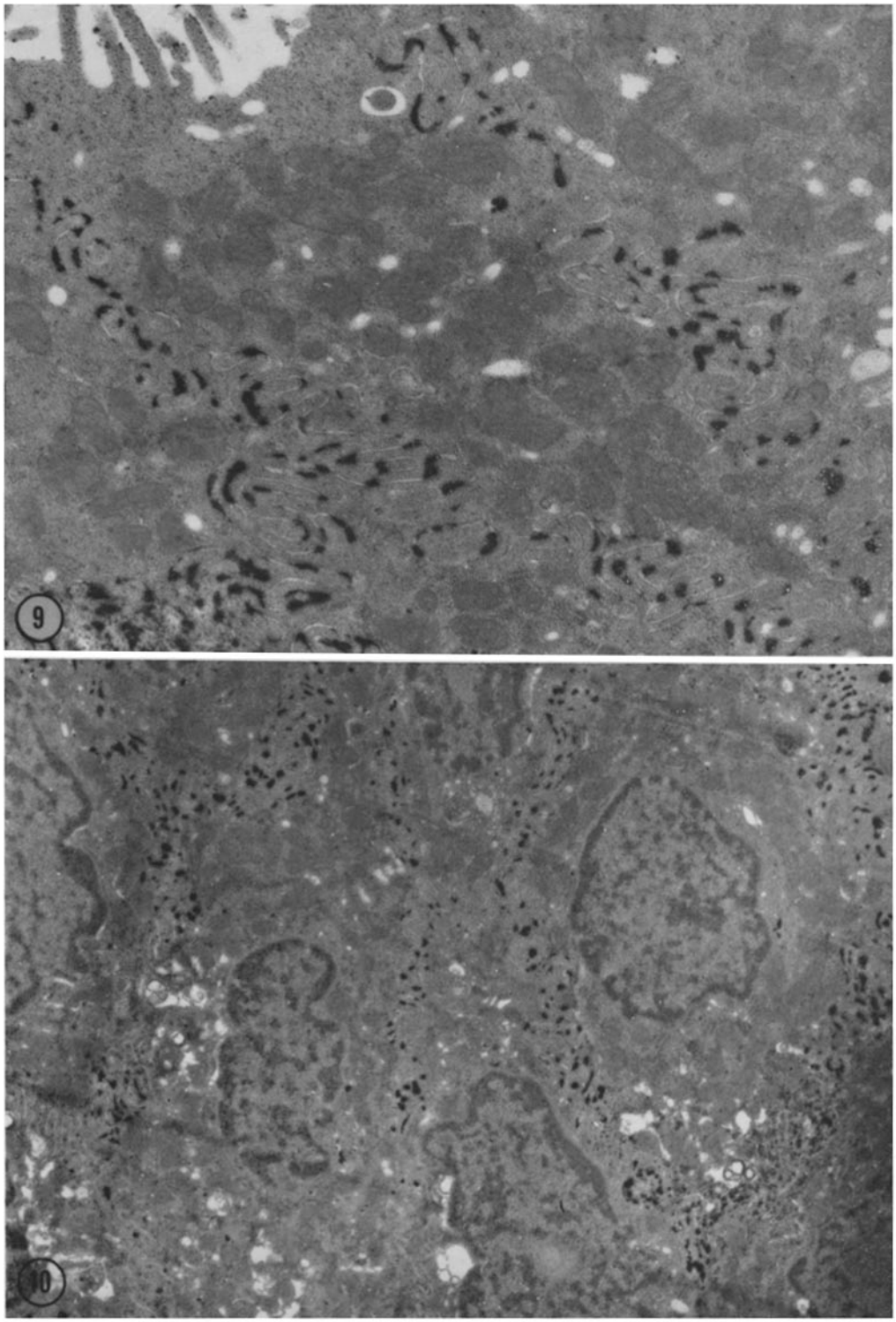

FIGURE 9 Apical ends of three epithelial cells from a gallbladder reacted for ATPase activity. The lead phosphate end product is restricted to the intercellular spaces and, when light, appears associated with the extracellular side of the lateral plasma membrane. × 26,000.

FIGURE 10 Cross-section at the nuclear level of the epithelium of the same bladder shown in Fig. 9. The lead phosphate end product of the ATPase reaction exactly outlines the lateral margins of the cells. × 13,500.

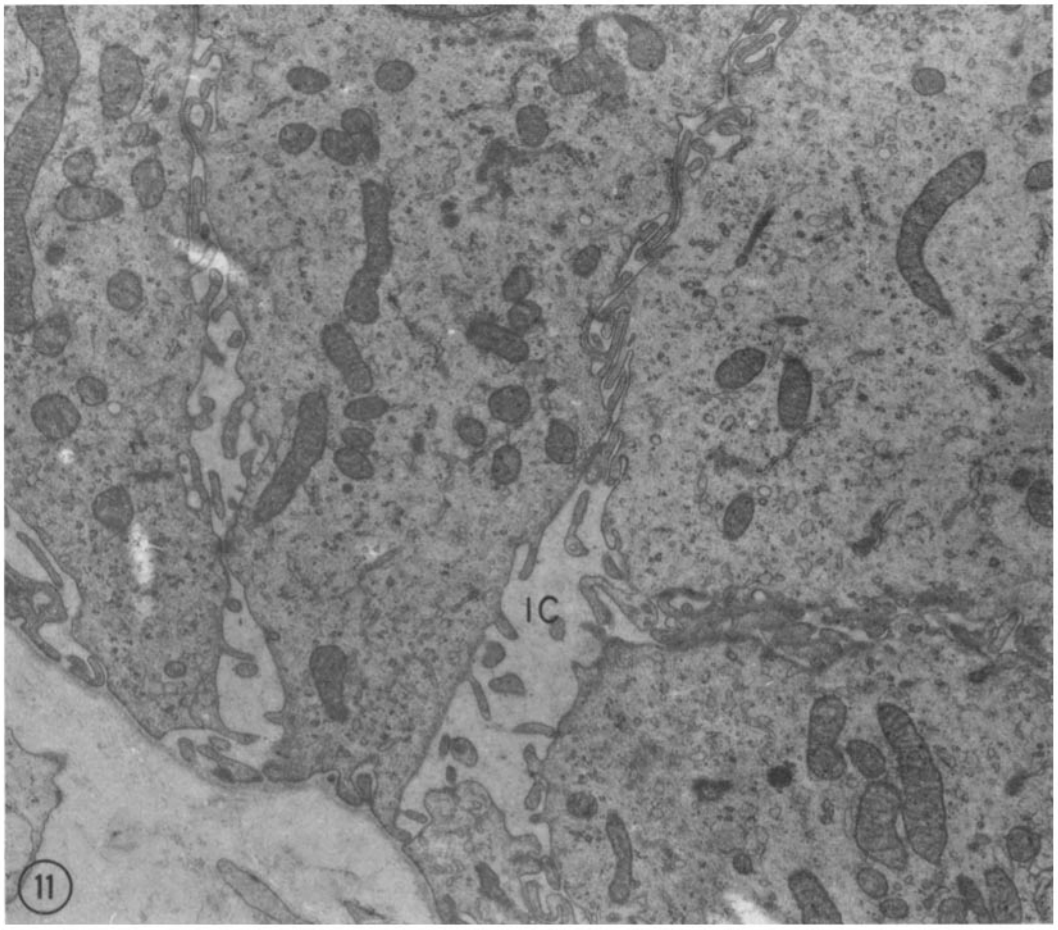

FIGURE 11 Basal end of several epithelial cells from a gallbladder dehydrating its bile in vivo at a rate of 550 μl/hr. The intercellular spaces (*IC*) are distended at their basal ends, but are maintained at 200 to 500 A immediately above the basal lamina by the close apposition of basal cell processes. × 13,500.

bathed in Na-free solution for approximately 30 min prior to fixation in the pyroantimonate-OsO_4 fixative, showed precipitate of $NaSb(OH)_6$ only in the intercellular spaces of the upper half of the mucosal folds, whether these spaces were approximately 200 A in width (Fig. 32 *a*) or distended (Fig. 32 *b*). No precipitate was seen in the cytoplasm of the cells of the upper half of the mucosal folds, but considerable precipitate was present in the lamina propria.

In the gallbladder from which 2 biopsies were taken prior to the addition of sodium to the mucosal bath, the biopsies, fixed in pyroantimonate-OsO_4, showed little or no precipitate in the cytoplasm or in the intercellular spaces (Fig. 26 *a* and *b*), which, as described above, were of approximately 200-A width except at the extreme crests of the mucosal folds. The lamina propria, in the first biopsy, showed precipitate mostly in the endothelium and lumen of capillaries and in the cytoplasm of fibroblasts. There was only a small amount of precipitate in the interstitial space. In the second biopsy, considerable precipitate was found in the lamina propria. One hour after sodium was added, the remainder of this bladder was fixed in the same fixative, and large particles of precipitate of $NaSb(OH)_6$ were found in the now distended epithelial intercellular spaces (Fig. 27). Small particles were found in the cytoplasm (Fig. 27). In the depths of the

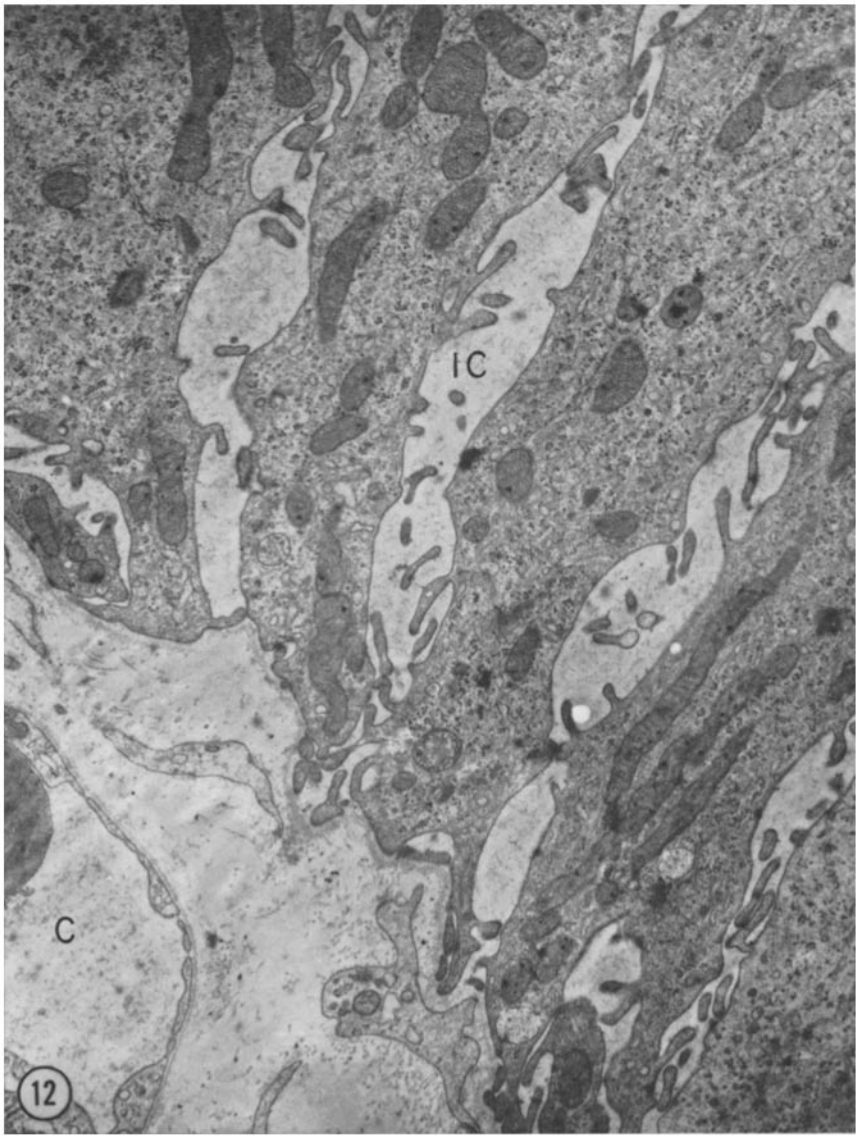

FIGURE 12 Basal portion of several epithelial cells from a gallbladder functioning in vivo with Krebs-Henseleit solution substituted for its bile (absorbing water from the lumen at a rate of 960 μl/hr). The distension of the intercellular spaces (*IC*) is much greater than in the bladder shown in Fig. 11, which was working at about half this rate. Note again, however, that the intercellular space is maintained at 200 to 500 A at the level of the basal lamina by the close apposition of the basal processes. A portion of a distended capillary (*C*) with attenuated fenestrated endothelium is also seen. × 15,000.

valleys, the area in which distension of the intercellular spaces has never been observed, there was little or no precipitate of $NaSb(OH)_6$ between the cells. The lamina propria, however, had many large particles of precipitate, particularly near the basal lamina (Fig. 27).

This series of experiments showed, therefore, that when transport was inhibited, the intercellular spaces were of approximately 200-A width at all levels of the mucosal folds. There was only occasional precipitate of $NaSb(OH)_6$ in the intercellular spaces and no precipitate within the

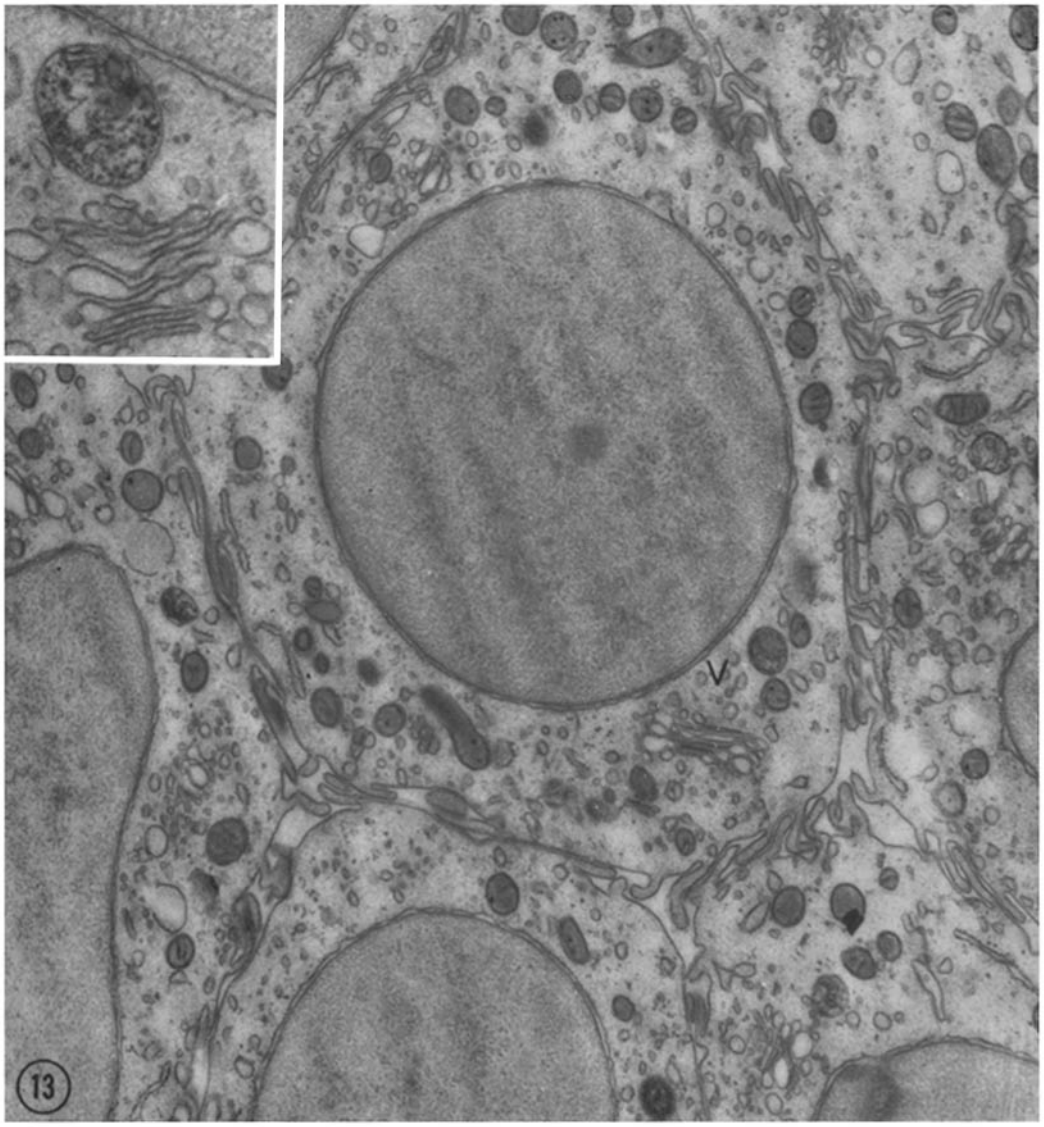

FIGURE 13 A cross-section at the nuclear level from the epithelium of the gallbladder shown in Fig. 12. Separation of the cells occurs at the points at which three or more cells would usually abut. Small vacuoles (*V*) containing accumulated ThO_2, which was presumably picked up by pinocytosis, are found near the Golgi zones of several cells (Inset). ×16,000; Inset, × 43,000.

cells. Distended intercellular spaces containing large precipitates of $NaSb(OH)_6$ and fine precipitate in the cytoplasm were found only after active fluid transport was initiated by addition of sodium.

DISCUSSION

Earlier studies of the gallbladder epithelium (9–12) described distension of the intercellular spaces as a regular structural feature and suggested that this distension might be related to the absorptive function of the gallbladder.

Our studies of 10 rabbit gallbladders obtained directly from the animals showed that the distension of the epithelial intercellular space was restricted to the upper levels of the mucosal folds and was not found in every gallbladder. The assumption that these variations were due to

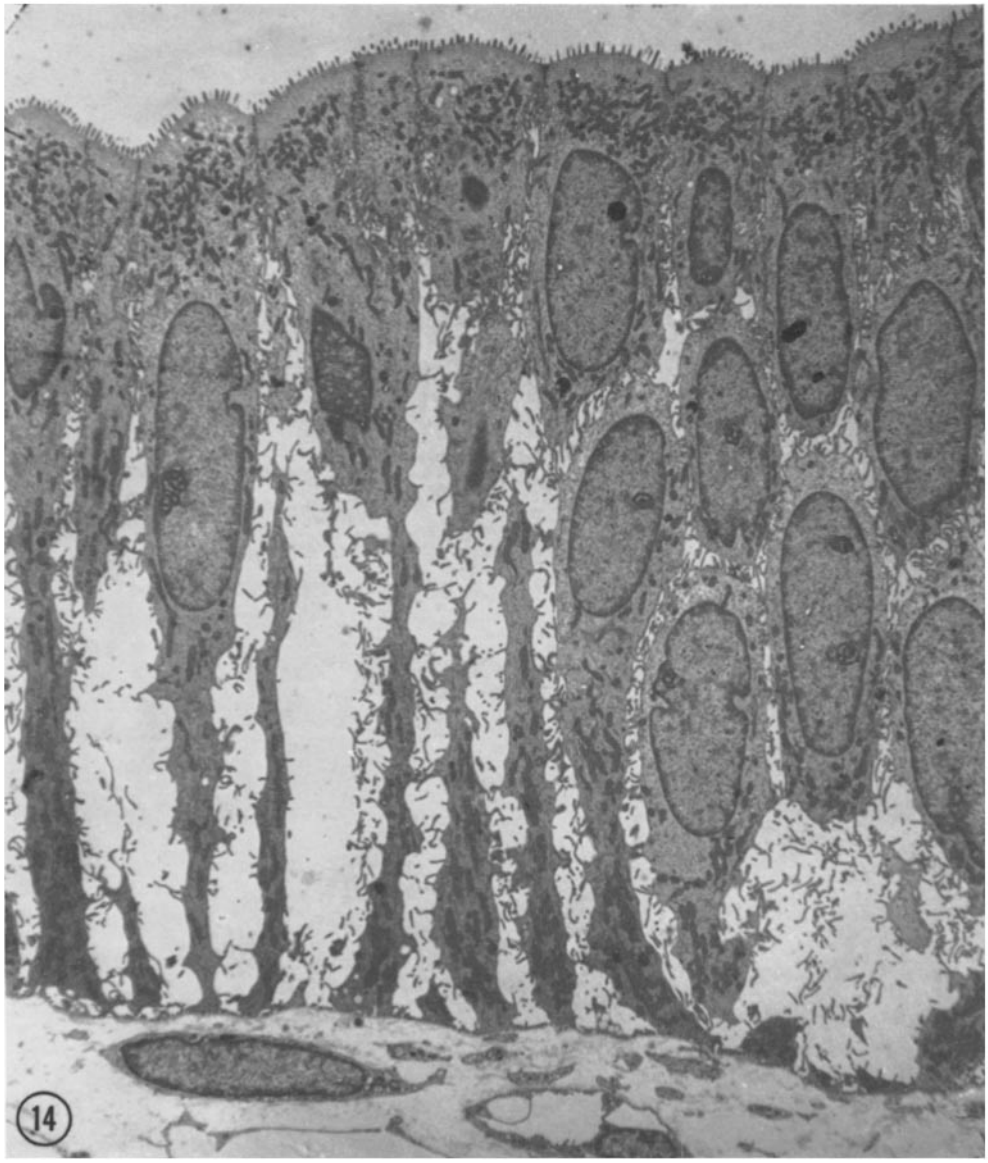

FIGURE 14 Low power electron micrograph of the epithelium of a gallbladder functioning in vitro showing the extreme degree to which the intercellular space can distend. However, the apical and basal relationships of the cells remain intact. × 2,100.

differences in functional state was confirmed by subsequent examination of bladders whose absorptive function was measured immediately prior to fixation. The intercellular spaces were distended in all bladders known to be absorbing water. When water flux was inhibited by an adverse osmotic gradient, there was a marked reduction in the size and number of distended intercellular spaces. When active solute transport was arrested by removal of sodium or chloride, the epithelial intercellular spaces were almost always of approximately 200-A width. The degree of distension was greater in functioning gallbladders studied in vitro than in those studied

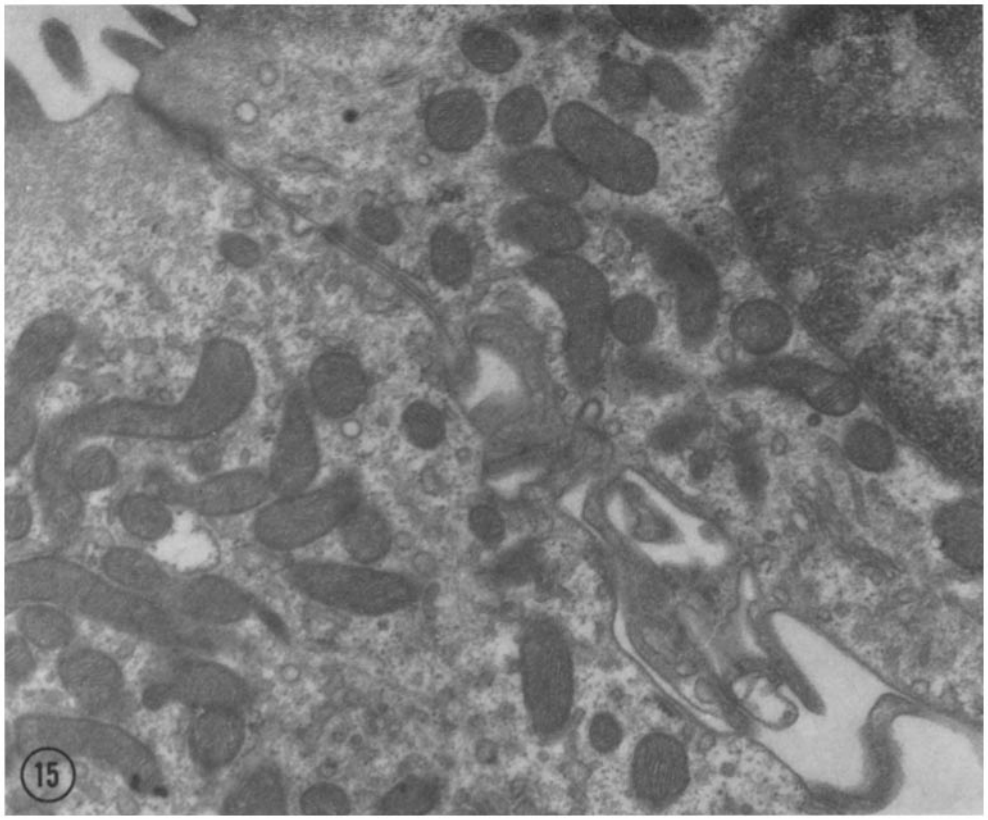

FIGURE 15 A portion of the apical end of two epithelial cells from a gallbladder functioning in vitro. The junctional complex appears to have its usual structure although the distension of the intercellular space extends to a point only a short distance below it. × 24,000.

in vivo, but the distribution of zones of intercellular distention within mucosal folds and the accompanying changes in the subepithelial structures were identical.

The belief that the distension of the intercellular spaces seen in the final image is an accurate picture of at least the relative volumes of tissue compartments at the time of fixation is justified on several grounds. Upon fixation with any of the fixatives used, the membranes lose their selective permeability and elasticity, assuming a semi-rigid condition which, although subject to some over-all shrinkage during dehydration, will be resistant to plastic deformation. If this were not the case, all cells, upon fixation, would tend to assume a spherical form. It is obvious that even red blood cells do not do this, but retain either their biconcave form or various shapes produced by packing in the lumina of blood vessels. In these studies, the relative form of the intercellular space did not vary with fixative used, fixation procedures, or tonicity or pH of the fixative over a wide range, but varied only with known functional state prior to fixation. This argues strongly that the distension of the intercellular spaces and subepithelial capillaries seen in the electron micrographs is a true picture of the presence of fluid in these spaces at the time of fixation.

The correlation between distension of intercellular spaces and active fluid absorption leaves little doubt that the intercellular compartment is traversed by the transported fluid. Although it is remotely possible that the edema of the lamina propria in vitro could produce distension of the intercellular spaces solely by reflux of fluid, this seems highly unlikely since significant distension was found in more than half of the bladders re-

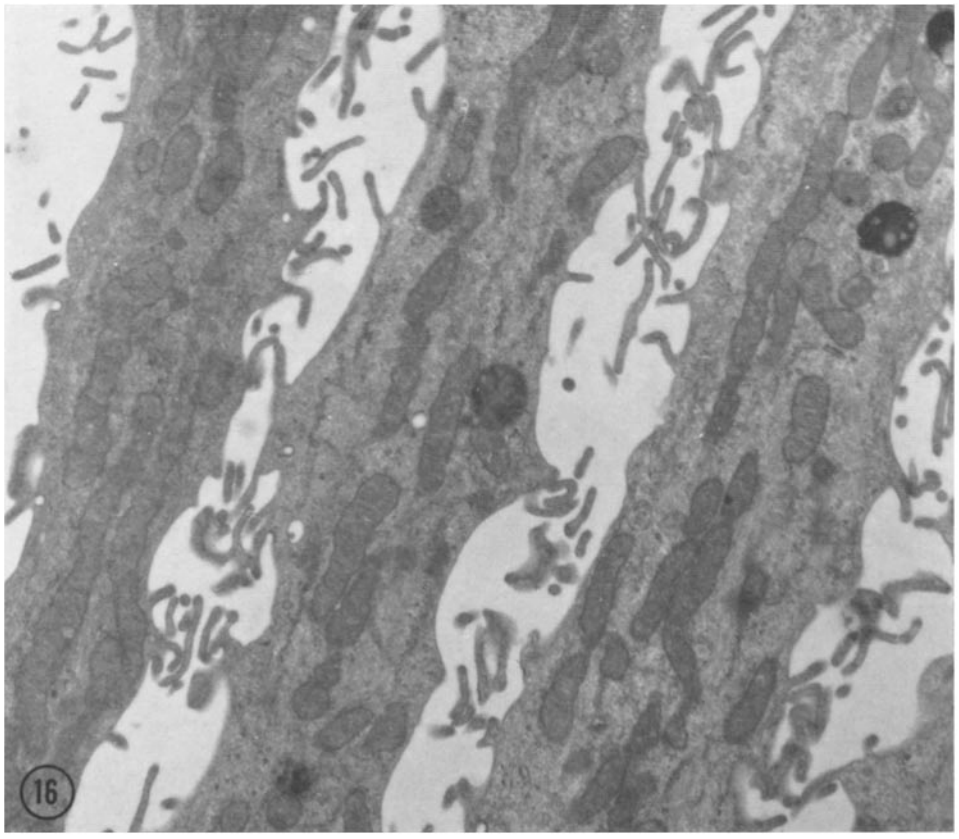

FIGURE 16 The midportions of the epithelial cells of gallbladders functioning in vitro appear as columns in a fluid compartment. The lateral plications and interdigitations seen in Figs. 3 and 4 appear here as lateral processes. × 12,500.

moved at random from apparently normal animals and in gallbladders known to be functioning in vivo, in which edema of the lamina propria was minimal or absent.

The pattern of precipitation of sodium pyroantimonate in gallbladders obtained directly from the animals and in bladders functioning in vitro also indicates that the intercellular compartment is part of the fluid pathway. Komnick (13) has shown, in artificial systems, that precipitation of large particles of $NaSb(OH)_6$ occurs at NaCl concentrations of the order of 0.9% (0.154 M). The finding of large particles of $NaSb(OH)_6$ in the distended intercellular spaces indicates that the fluid in these spaces, in contrast to the intracellular fluid, has a high Na^+ concentration. This is consistent with the known composition of transported fluid (5). The virtual absence of precipitate from the epithelial cells and interstitial spaces of bladders bathed in Na-free media shows that the presence of pyroantimonate precipitate in these regions can be equated, specifically, to the presence of sodium.

Physiological studies of the rabbit gallbladder (4–8) have shown that it exhibits characteristics which would be predicted by analysis of the Curran serial membrane model (21–23). A schematic representation of this model is shown in Fig. 33 (left). The model describes the transporting system as composed of three compartments in series, separated by two barriers (membranes). Barrier *1* (which separates compartments *l* and *m*) is assumed to be a semipermeable membrane in the model system, and in actual systems is also presumed to be the site of active solute transport in the direction *l* to *m*. Barrier *2* is defined

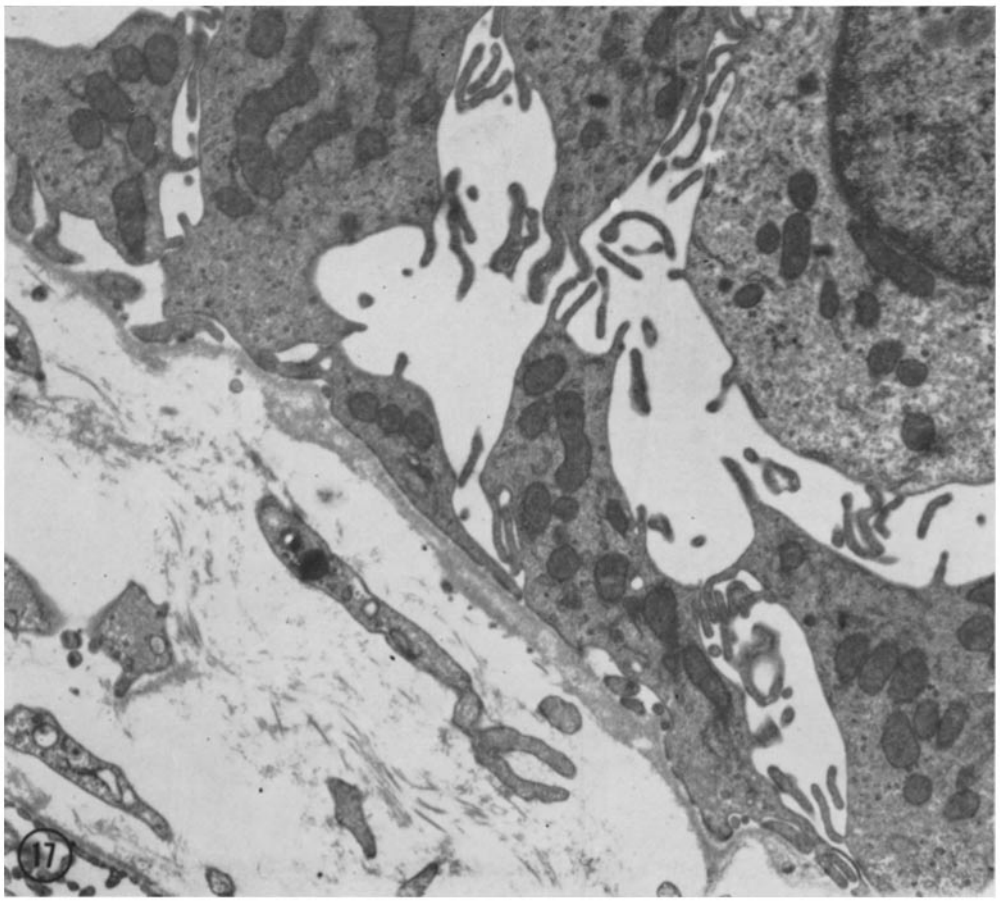

FIGURE 17 At the basal end, the close apposition of basal processes is maintained, as is the relationship between the cells and the basal lamina, despite the extreme distension of the intercellular space in gallbladders functioning in vitro. × 12,500.

by Curran as a nonselective barrier which merely retards diffusion of solutes between compartments *m* and *r*.

This model can account for transport of water (coupled solute-solvent transport) in the following manner: Active transport of solute occurs across barrier *1*, increasing the concentration of solute in the middle compartment (*m*). Because of the resulting osmotic gradient across semipermeable barrier *1*, water moves from compartment *l* into compartment *m*. This leads to the development of a hydrostatic pressure in the middle compartment which drives solution across barrier *2* into compartment *r*. The net effect of this process is the transport of both solvent and solute from compartment *l* to compartment *r* in response to active solute transport, and the model has actually been shown to be capable of transporting water "uphill" (22, 23).

Patlak, Goldstein, and Hoffman (24) have presented a general mathematical description of the serial membrane system. Based on their description, it has been possible to show that all of the observed characteristics of coupled solute-solvent transport by the gallbladder, together with its unusual electrical behavior, are explainable by the operation of such a system within the gallbladder epithelium (8).

The morphological data and theoretical considerations immediately suggest that the intercellular compartment is directly analogous to the middle compartment of the serial membrane

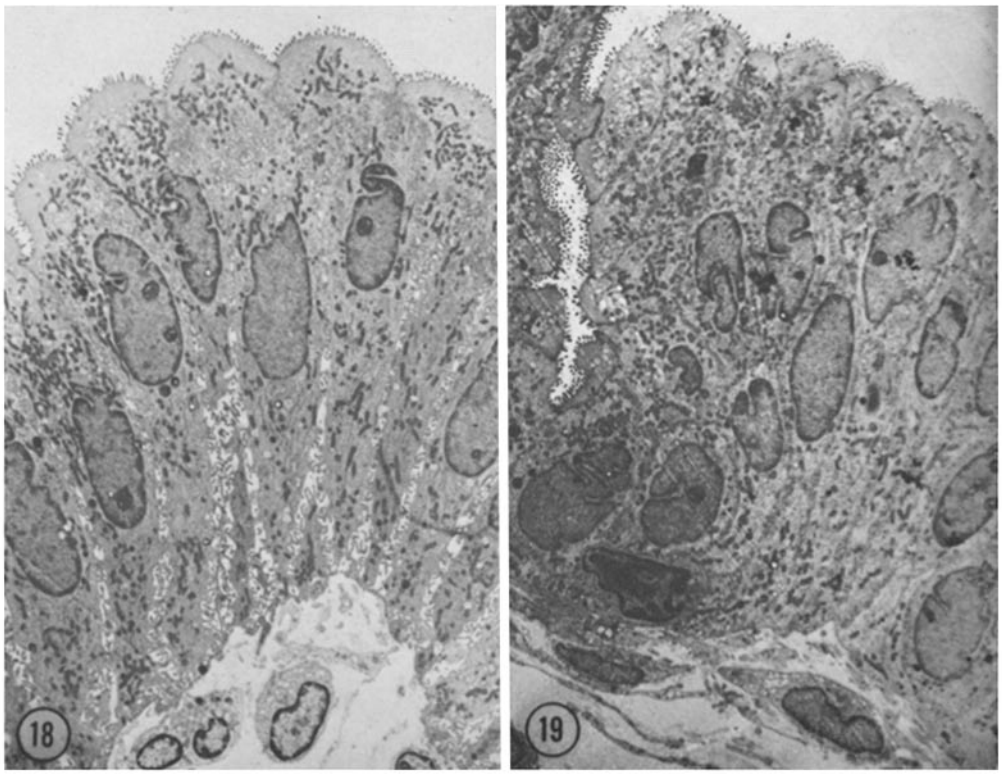

FIGURES 18 and 19 A hyperosmotic solution in the lumen reduced the net water flux in this gallbladder to less than 15 μl/hr. Under these conditions, the intercellular spaces at the crests of some of the mucosal folds (Fig. 18) were moderately distended while those near the crest (Fig. 19) or on other crests were not distended. × 1,400.

system. A diagrammatic representation of the rabbit gallbladder wall, appropriately labeled to show the analogy between its structure and the Curran model, is seen in Fig. 33 (right). The intercellular compartment is bounded on one side by a semipermeable membrane, the lateral plasma membrane of the epithelial cells, and on the other side by a diffusion barrier, the epithelial basal complex (25), consisting of the narrow channel at the basal end of the intercellular space, the epithelial basal lamina, the thin underlying portion of the lamina propria, and (in gallbladders with an intact vascular supply) the basal lamina and endothelium of the subepithelial capillaries.

The distension of the intercellular spaces observed during active fluid absorption in the gallbladder must be due to the development of a positive hydrostatic pressure in this compartment, analogous to the positive pressure which must develop in the middle compartment of the functioning serial membrane model. The analogy would further require that the lateral plasma membrane of the epithelial cells, as the first barrier, must be the site of active solute transport into the middle (intercellular) compartment. While actual sites of active solute transport in the gallbladder epithelium cannot be identified at this time, the cytochemical observation that the concentration of the major transported cation, sodium, is much higher in the intercellular than in the intracellular fluid is, at least, consistent with the view that active transport of electrolyte may occur at the lateral plasma membrane. In addition, the localization of ATPase activity at this membrane suggests a parallel between the lateral cell membrane of the gallbladder epithelium and those of the frog skin (26), colon (27), amphibian urinary bladder (28), corneal endothelium and epithelium (29), mammalian kidney tubule (30, 31), and ciliary epithelium (32)

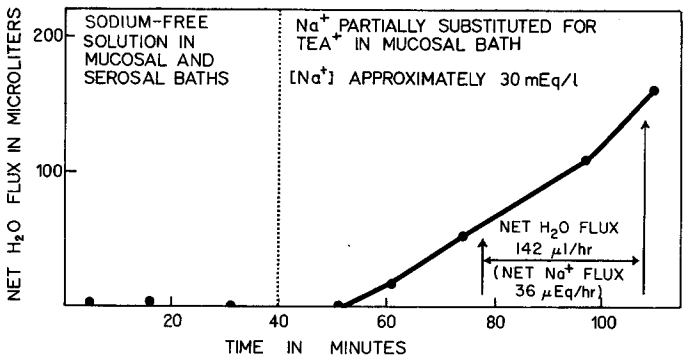

FIGURE 20 Substitution of tetraethylammonium for sodium in the mucosal and serosal baths completely arrests water transport across the wall of the gallbladder. Addition of some sodium to the mucosal bath leads to vigorous transport of both NaCl and water.

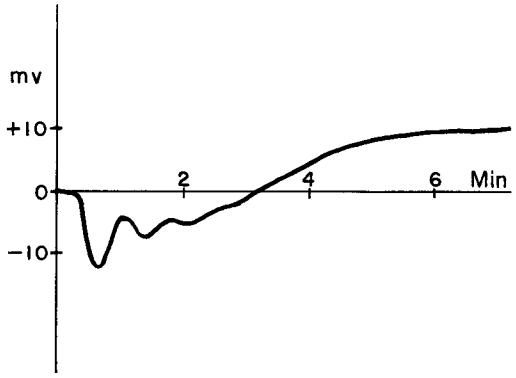

FIGURE 21 Continuous recording of electrical potential in mucosal bath relative to serosal bath following addition of sodium to mucosal fluid. Agar bridges composed of Na-free solution (serosal) and 3 M KCl (mucosal) were connected through calomel cells to a Keithley Model 600A electrometer and Varian Model G-14A2 recorder. The bladder was bathed initially in Na-free solution. At time zero, mucosal Na concentration was increased from zero to approximately 30 mEq/l. The lumen was initially negative, owing to diffusion of sodium ions toward the serosa. The early undulations are artifacts due to incomplete mixing in the mucosal fluid. The subsequent change to positive potential can be attributed to back diffusion of sodium accumulated in the subepithelial layer resulting from active NaCl transport. This potential change suggests that rapid transport began within 3 min of the time sodium was added to the lumen.

in which localization of ATPase activity appears to be associated with electrolyte transport.

However, it is obvious that the biological system is not so simple as the model. Assuming that the cells are tightly joined together by the apical junctional complex, the lumen of the gallbladder is separated from the intercellular compartment by the apical plasma membrane, cytoplasm, and lateral plasma membrane of the epithelial cells. Fluid which is transported across the lateral surface of the cells into the intercellular compartment would have to be replaced by movement of fluid into the cells through some other surface. This movement would have to occur preferentially across the apical rather than basal surface of the cell in order to accomplish net transmural fluid transport. Although the relative permeability of the apical and basal surfaces is unknown, it is at least obvious that the area available for diffusion at the microvillous luminal surface is much greater than that at the basal surface.

The proposed location of the third (r) compartment (Fig. 33) is different in the bladder whose blood supply is intact than it is in the bladder studied in vitro. In the gallbladder in vivo the vascular compartment (Fig. 33, r) is the third compartment. In gallbladders studied in vitro, the serosal bath (Fig. 33, r') is made the third compartment by virtue of the experimental design; hence, the theoretical second barrier in vitro must include the entire thickness of the lamina propria, muscularis, subserosa, and serosa and must, therefore, necessarily impose a greater resistance to fluid movement. In the serial membrane model, an increase in the resistance of the second barrier to hydrostatic filtration would be accompanied by a diminution in the rate of fluid transport and an increase in the hydrostatic pressure in the middle compartment (22–24). This would provide a theoretical explanation

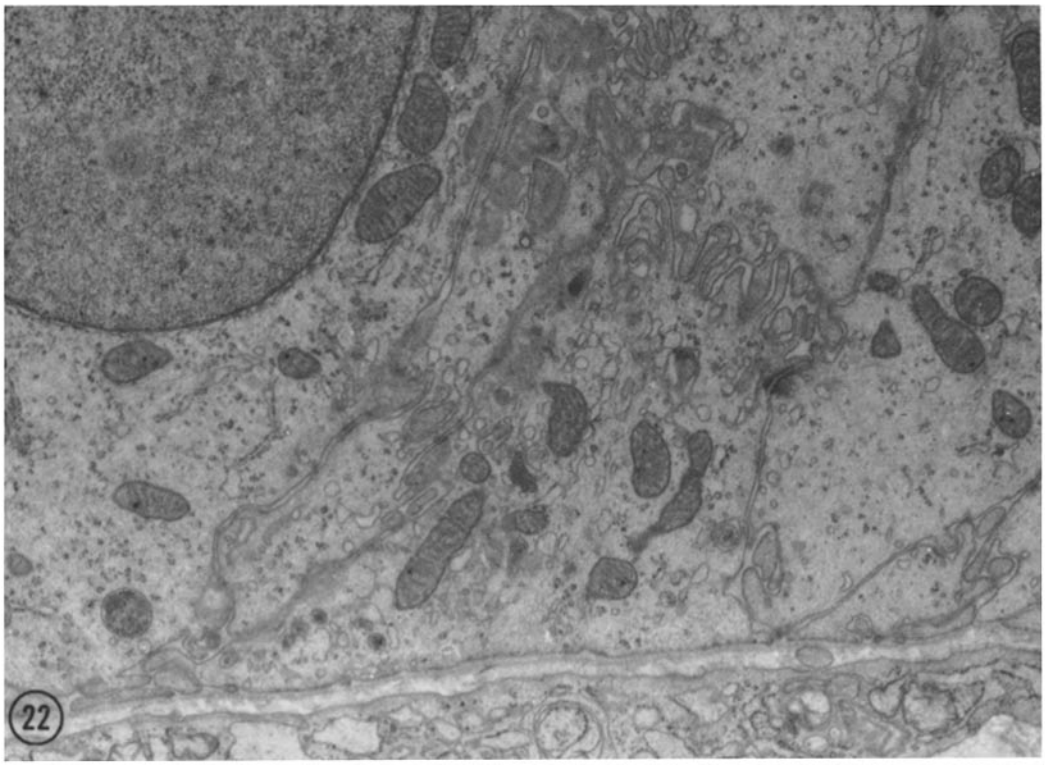

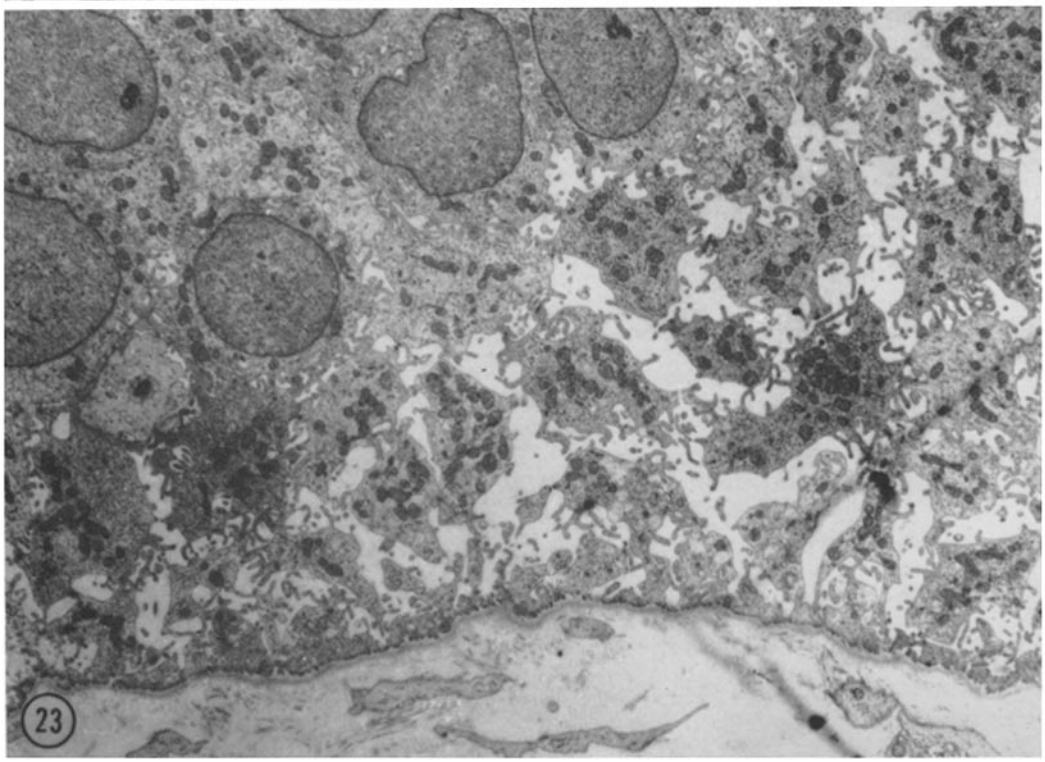

FIGURES 22 and 23 Basal ends of epithelial cells from the side (Fig. 22) and crest (Fig. 23) of a mucosal fold from the fundus of a gallbladder biopsied while in sodium-free solution. There is no distension of the intercellular spaces on the side of the fold (Fig. 22) and only moderate distension at the extreme crest (Fig. 23). Fig. 22, × 14,400; Fig. 23, × 6,000.

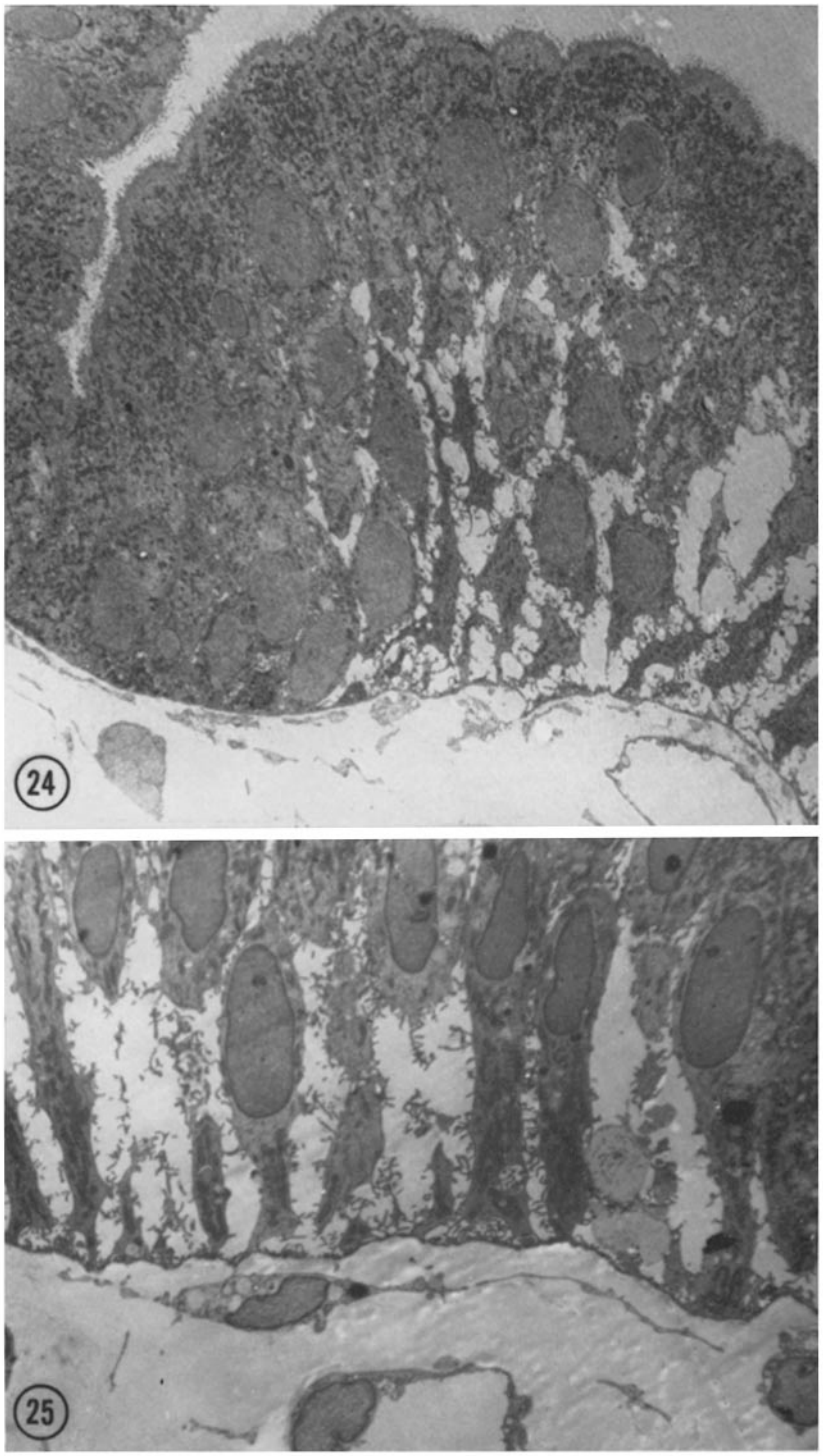

FIGURES 24 and 25 Low power electron micrographs of the epithelium of the same gallbladder shown in Figs. 22 and 23 fixed after transport was reestablished by the addition of sodium to the mucosal bath. Extreme distension of the intercellular spaces is now found along the entire length of each fold. Fig. 24 shows the last cobble before the depth of a valley (at the left) and Fig. 25 shows the crest of the same fold. (Compare with Figs. 22 and 14). Fig. 24, × 1,300; Fig. 25, × 1,700.

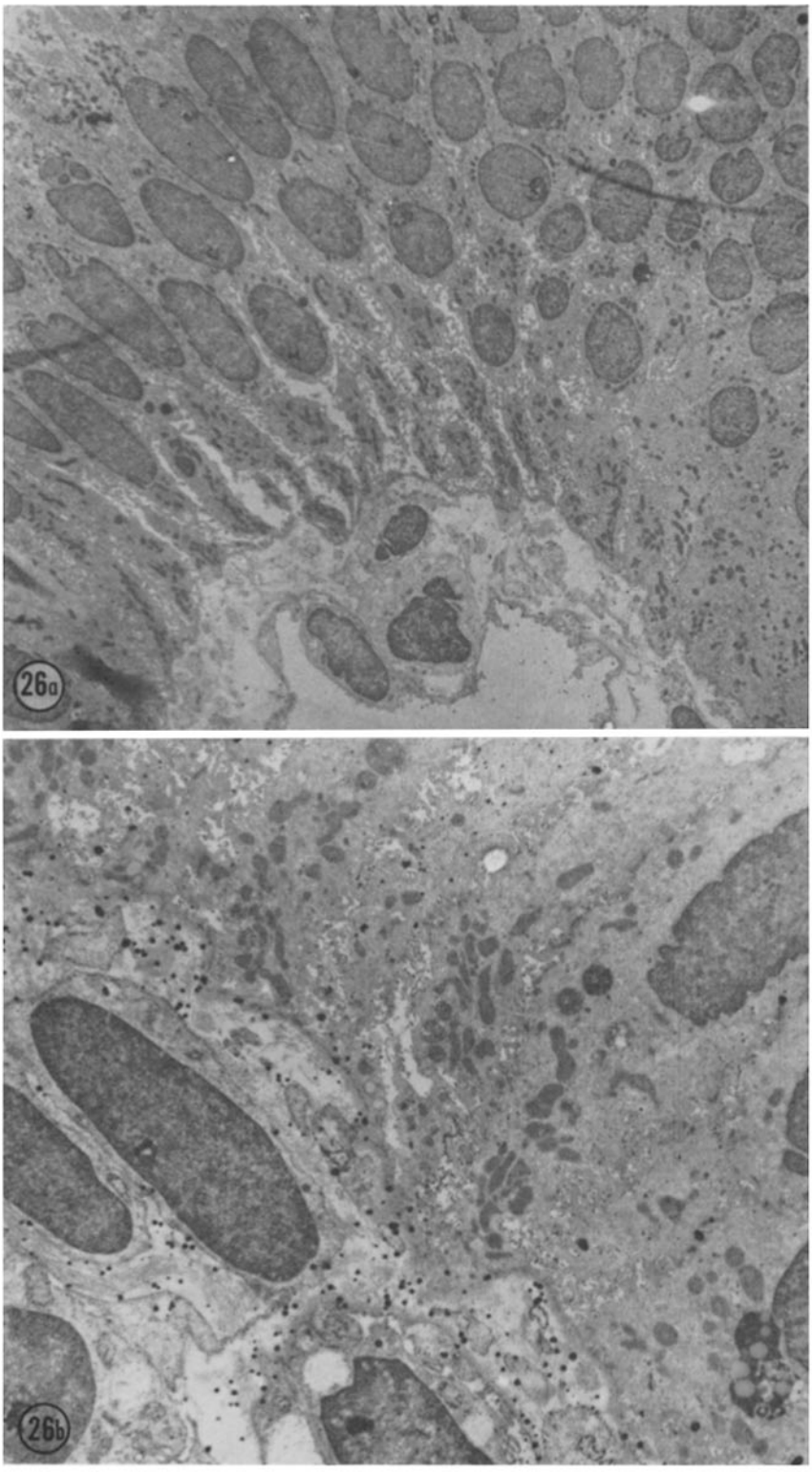

FIGURE 26 This figure shows tissue from biopsies taken at 15 min (*a*) and 85 min (*b*) in Na-free media (net water flux of zero). Distension, which is slight, is found only at the extreme crests of mucosal folds at both time points. These biopsies, fixed in the pyroantimonate-OsO_4 mixture, show no precipitate of $NaSb(OH)_6$ in the intercellular space (or cells) at 15 min (*a*) and only slight precipitate in the spaces at 85 min (*b*). At both time points, precipitate is found in the lamina propria, often closely subjacent to the basal lamina. Fig. 26 *a*, × 1,700; Fig. 26 *b*, × 4,600.

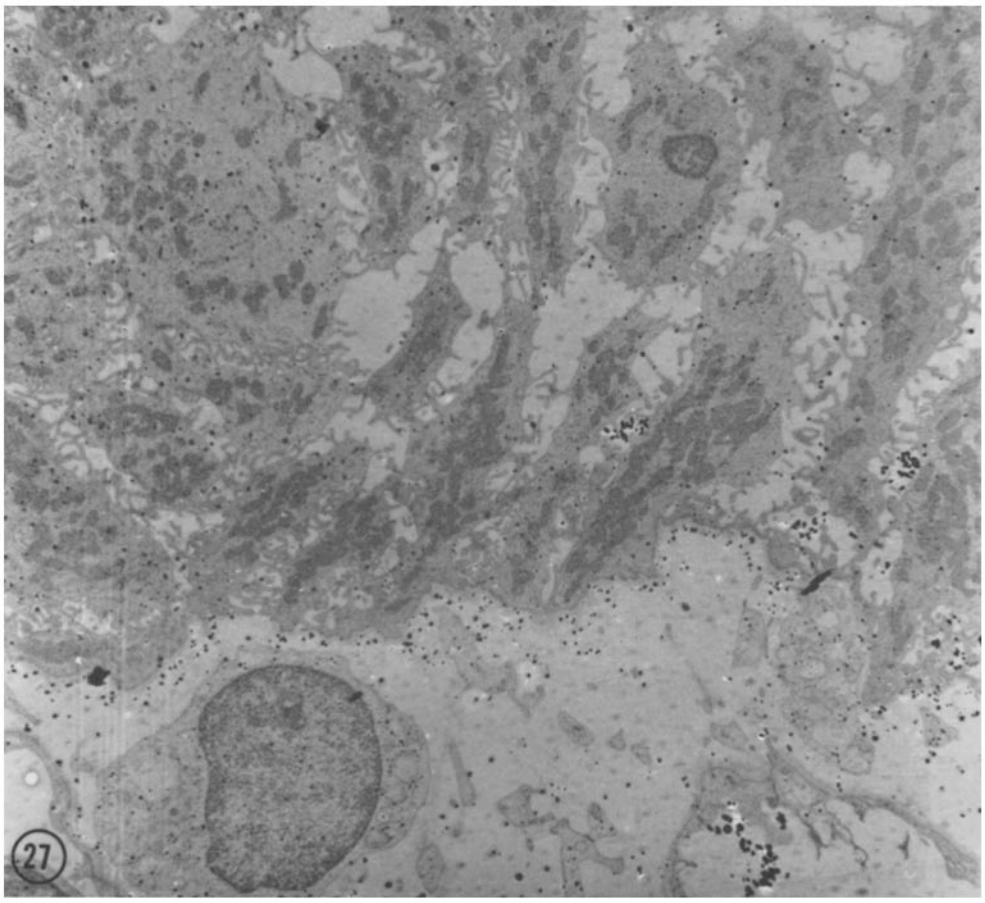

FIGURE 27 The crest of a mucosal fold from the remainder of the same bladder shown in Fig. 26 fixed 60 min after the addition of sodium to the mucosal bath. Large particles of $NaSb(OH)_6$ are found in the distended intercellular spaces as well as in the lamina propria, particularly just beneath the basal lamina, and small particles are found in the cytoplasm of the epithelial cells. × 4,100.

for the lower rates of fluid absorption measured in vitro than in vivo as well as the relatively greater distension of the intercellular spaces found in the bladders studied in vitro.

The changes which occur in the structure of the subepithelial capillaries (Figs. 4 to 6, 12, 28, 29) as well as the close functional relationship between the capillaries and the epithelium (Figs. 4 to 6, 8, 12, 28, 29) further attest to the importance of the vascular system in the total transport process in the living animal.

Until recently, despite the fact that transporting and secreting systems were among the first tissues examined with the electron microscope (33–43), only observations of increased cell surface area or studies of pinocytosis in these systems had been made using this instrument. In part, the present studies were undertaken to reexamine Hayward's (44) observation of the pinocytotic uptake of ThO_2 by the gallbladder epithelium of the guinea pig. We have been unable to demonstrate transepithelial transport of colloidal particles by pinocytosis in the gallbladder epithelium. Although there is some uptake and sequestering of ThO_2, no marker appears to cross the cellular layer. Thus, there is no direct evidence to support the hypothesis advanced by Grim (45) that the net transport of solute and and solvent by the gallbladder can be accounted for by pinocytosis. Even in the rabbit corneal

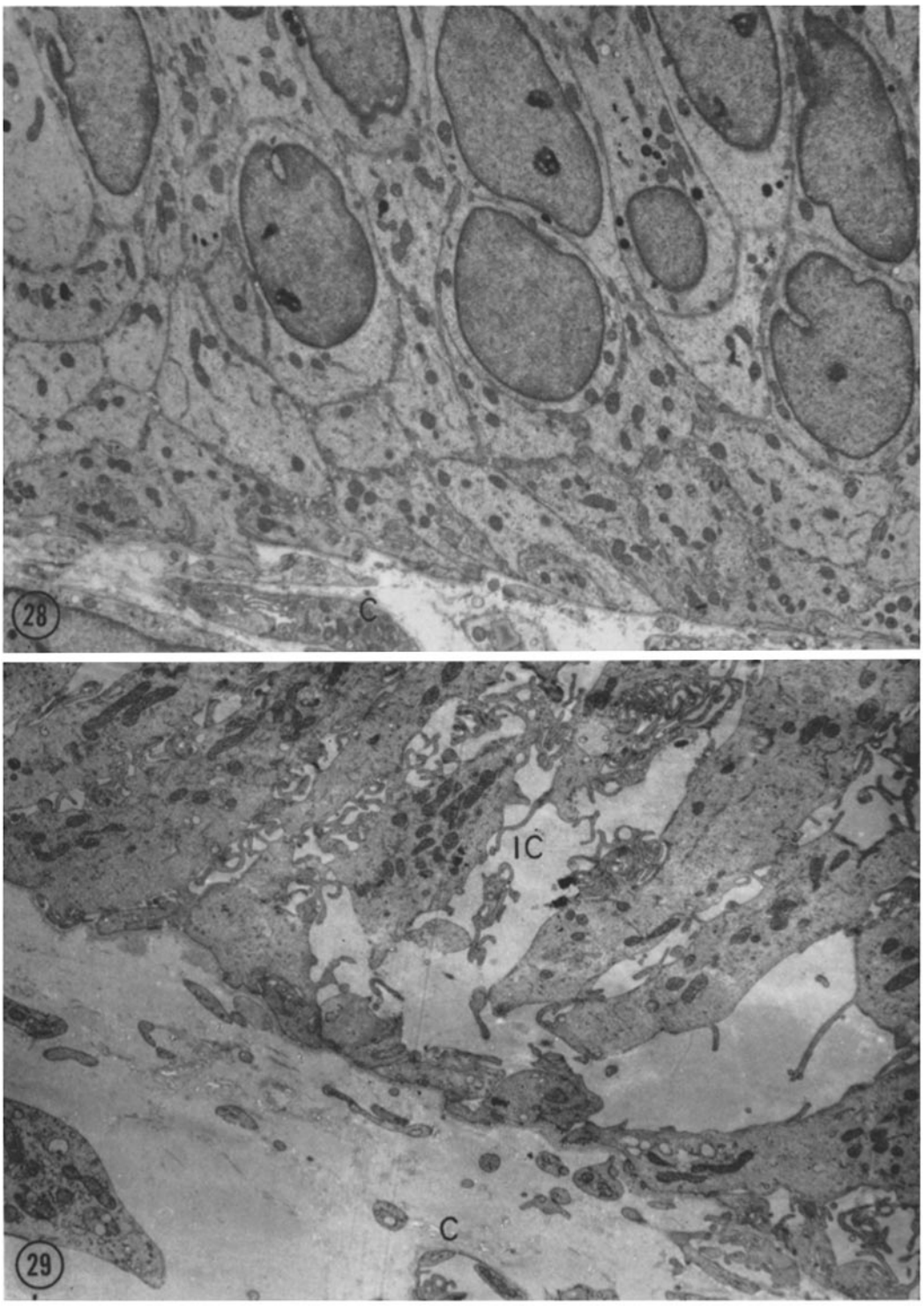

FIGURES 28 and 29 Substitution of sulfate for chloride similarly inhibits solute and water transport. In the nonworking state (Fig. 28) the epithelial intercellular spaces are not distended, nor are the capillaries (*C*). In a comparable area from the same bladder fixed after solute and solvent transport was reestablished by the addition of a NaCl-$NaHCO_3$ solution (Fig. 29), there is considerable distension of the intercellular spaces (*IC*). The capillaries (*C*) of the lamina propria are also distended. Fig. 28, × 6,200; Fig. 29, × 4,600.

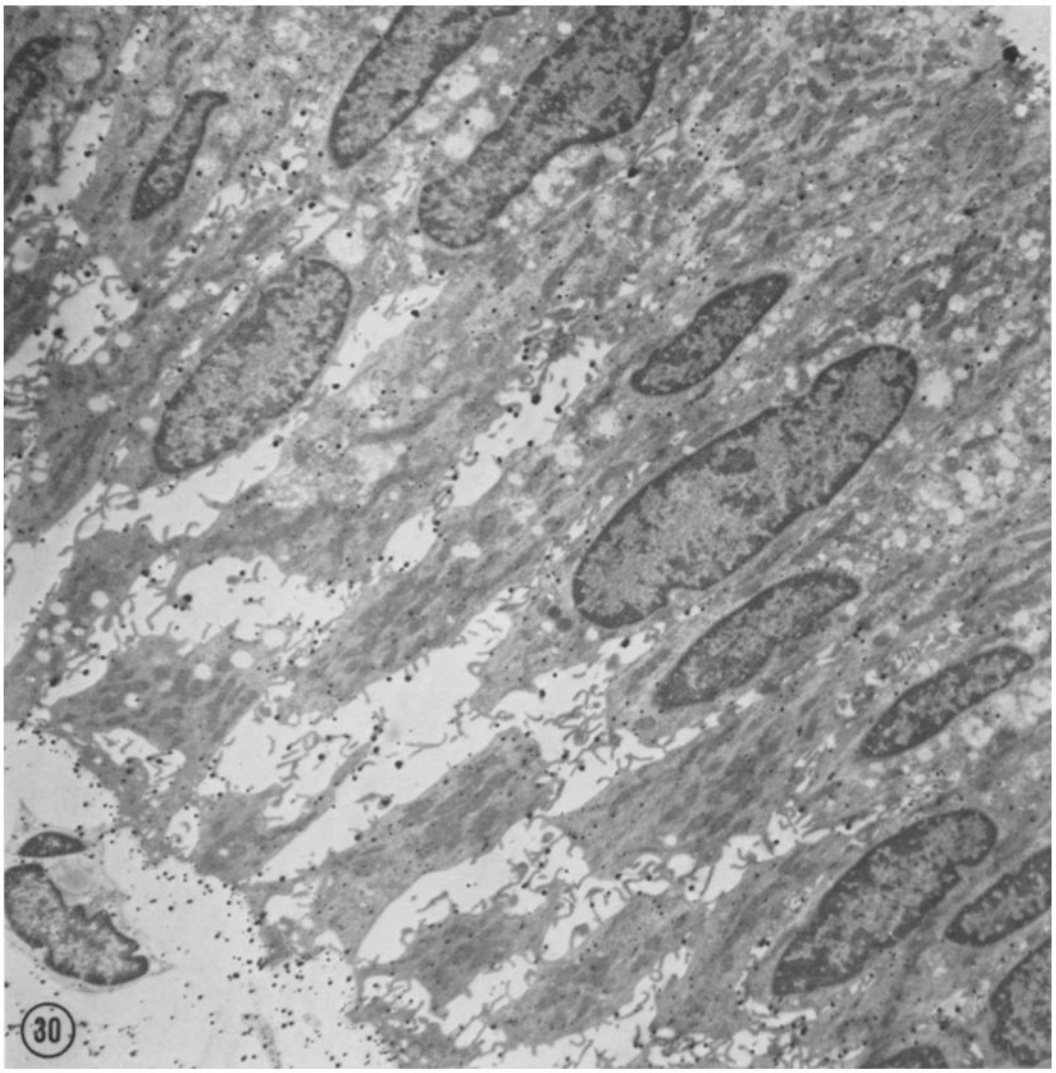

FIGURE 30 Portion of the epithelium of a gallbladder functioning in vitro fixed in the pyroantimonate-OsO_4 mixture. Large particles of $NaSb(OH)_6$ are found throughout the distended intercellular spaces, indicating a high concentration of sodium in these spaces in the functioning gallbladder. Large particles of precipitate are also found in the lamina propria. Small particles are found in the cytoplasm of the epithelial cells. × 4,600.

endothelium (46–48), one of the few systems in which pinocytosis has been shown to be a true transepithelial transport system, rather than an absorptive system, it has recently been suggested (49, 50) that the pinocytotic vesicles are dependent for their directed movement on a sodium or ionic pump system in the lateral cell membrane of the corneal endothelial cell.

During the studies of pinocytosis in the corneal endothelium, distension of the intercellular space was observed, but unexplained (46–48). The literature of the fine structure of transporting and absorptive epithelia contains numerous studies in which distension of the intercellular space was shown, but usually not commented on (39–41, 51–58, 60, 61). Some authors, however, have drawn attention to this space (9–12, 60, 61). Hayward (10, 59) has even drawn the parallel

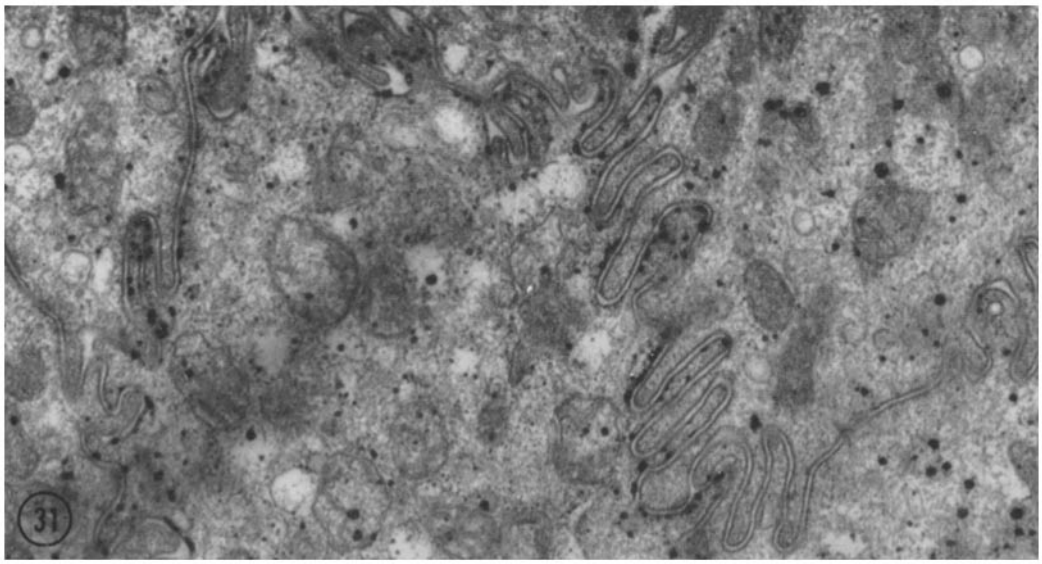

FIGURE 31 In the apical portion of the epithelium, in some areas in which the intercellular spaces were not distended, $NaSb(OH)_6$ was localized on the intracellular side of the lateral plasma membrane. × 28,000.

between the fine structure of the mucosae of the gallbladder and colon (59) and suggested that this structure was related to their fluid absorptive function. Studies in our own laboratory (25) have shown that the intercellular spaces of the epithelium as well as the structure of the subepithelial capillaries of the ileum and colon are subject to the same variations, relative to functional state, as those of the gallbladder. Carasso et al. have made similar suggestions on the importance of the intercellular space in transepithelial transport, following studies on hormonal effects on transport in the toad bladder (60). We believe, therefore, that the analogy drawn above between the Curran serial membrane model and the fine structure of the rabbit gallbladder may be generally applicable to transport across many epithelia and may help to interpret the structural-functional relationships in other transporting tissues.

This study was supported in part by Grants GM-11343, AM-07228 and AM-07374 of the National Institutes of Health, United States Public Health Service, and by Grant P-362 of the American Cancer Society, Inc. Dr. Kaye is the recipient of a Career Scientist Award of the Health Research Council of the City of New York under Contract I-320. During part of the period of this study, Dr. Whitlock was a Senior Postdoctoral Fellow of the New York Heart Association.

The authors are indebted to Mrs. Jeanne D. Cole, Mrs. Elizabeth Ross, Mrs. Maria Rivera, and Mrs. Linda F. Siegel for their invaluable assistance in these studies.

Received for publication 14 January 1966.

REFERENCES

1. DIAMOND, J. M., The reabsorptive function of the gallbladder, *J. Physiol. (London)*, 1962, **161**, 442.
2. DIAMOND, J. M., The mechanism of solute transport by the gall-bladder, *J. Physiol. (London)*, 1962, **161**, 474.
3. DIAMOND, J. M., The mechanism of water transport by the gall-bladder, *J. Physiol. (London)*, 1962, **161**, 503.
4. WHITLOCK, R. T., MANCUSI-UNGARO, P. L., and WHEELER, H. O., Effect of osmolality on water absorption by the gallbladder, *Fed. Proc.*, 1963, **22**, 622.
5. WHEELER, H. O., Transport of electrolytes and water across wall of rabbit gall bladder, *Am. J. Physiol.*, 1963, **205**, 427.
6. DIAMOND, J. M., Transport of salt and water in rabbit and guinea pig gall bladder, *J. Gen. Physiol.*, 1964, **48**, 1.

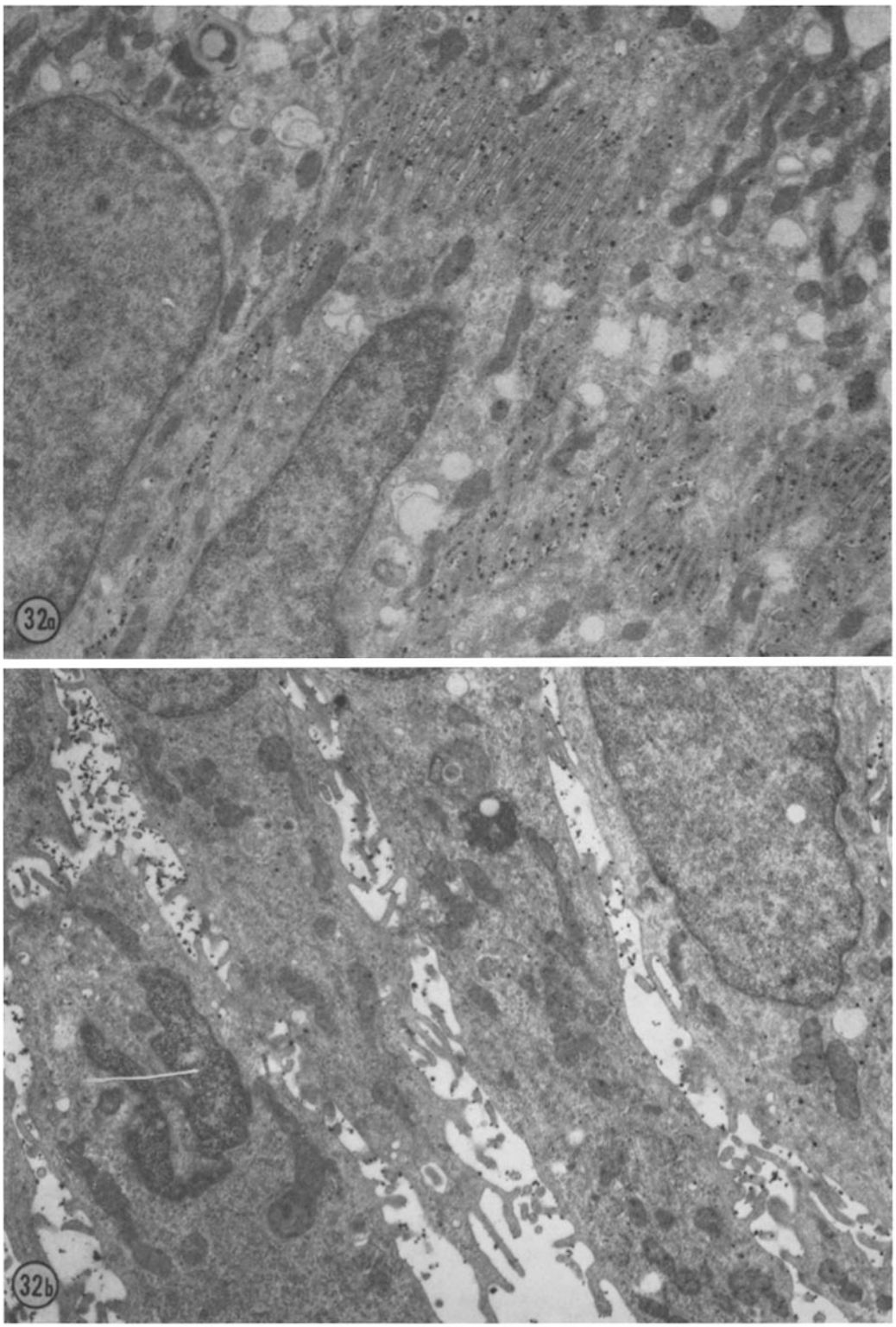

FIGURE 32 Portions of the epithelium from a gallbladder which had been bathed in Na-free solution for approximately 30 min prior to fixation in the pyroantimonate-OsO_4 mixture. In this case, $NaSb(OH)_6$ was found almost exclusively in the intercellular spaces, whether they were of approximately 200-A width (*a*) or distended (*b*). A small amount of precipitate was found in vesicles in the cytoplasm, but the extensive cytoplasmic deposition of small particles found in actively absorbing bladders (Fig. 30) was absent. This suggests that the bladder continued to pump solute into the space from the cells until the available solute was exhausted. × 13,500.

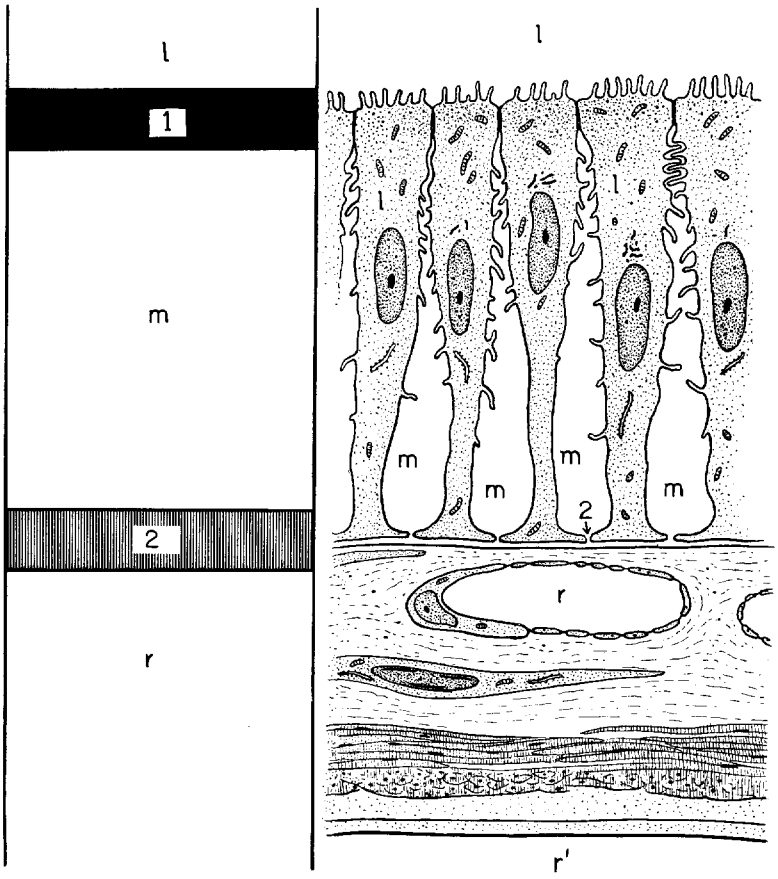

FIGURE 33 Schematic representation of the Curran serial membrane model (left) and of the wall of the rabbit gallbladder (right). The Curran model is composed of three compartments in series, separated by two barriers (membranes). Barrier *1* (which separates compartments *l* and *m*) is assumed to be a semipermeable membrane in the model system, and in actual systems is also presumed to be the site of active solute transport in the direction *l* to *m*. Barrier *2* is defined by Curran as a nonselective barrier which merely retards diffusion of solutes between compartments *m* and *r*. This model can account for net transport of water (coupled solute-solvent transport (see text)).

On the right, a diagrammatic representation of the rabbit gallbladder wall is appropriately labeled to show the analogy between its structure and the Curran model.

The intercellular space fulfills all the requirements of the middle compartment. In vivo, the epithelial basal complex (25), consisting of the narrow channel, the basal lamina of the epithelium, the small amount of lamina propria, and the basal lamina and capillary endothelium, is the second barrier and the vascular compartment is the *r* compartment. In vitro, the serosal bath is made the third compartment (*r'*) by virtue of the experimental design. Hence the second barrier must include the entire thickness of the wall of the gallbladder beneath the epithelium.

7. DIAMOND, J. M., The mechanism of isotonic water transport, *J. Gen. Physiol.*, 1964, **48**, 15.
8. WHITLOCK, R. T., and WHEELER, H. O., Coupled transport of solute and water across rabbit gallblader epithelium, *J. Clin. Invest.*, 1964, **43**, 2249.
9. YAMADA, E., The fine structure of the mouse gall bladder epithelium, *J. Biophysic. and Biochem. Cytol.*, 1955, **1**, 455.
10. HAYWARD, A. F., Aspects of the fine structure of the gall bladder epithelium of the mouse, *J. Anat. (London)*, 1962, **96**, 227.
11. JOHNSON, F. R., MCMINN, R. M. H., and BIRCHENOUGH, R. F., The ultrastructure of

the gall-bladder epithelium of the dog, *J. Anat. (London)*, 1962, **96**, 477.

12. EVETT, R. D., HIGGINS, J. A., and BROWN, A. L. JR., The fine structure of normal mucosa in human gall bladder, *Gastroenterology*, 1964, **47**, 49.
13. KOMNICK, H., Elektronenmikroskopische Lokalisation von Na^+ und Cl^- in Zellen und Geweben, *Protoplasma*, 1962, **55**, 414.
14. WACHSTEIN, M., and MEISEL, E., Histochemistry of hepatic phosphatases at a physiologic pH with special reference to the demonstration of bile canaliculi, *Am. J. Clin. Path.*, 1957, **27**, 13.
15. KREBS, H. A., and HENSELEIT, K., Untersuchungen über die Harnstoffbildung in Tierkorper, *Hoppe-Seylers Z. physiol. Chem.*, 1932, **210**, 33.
16. LUFT, J. H., Improvements in epoxy resin embedding methods, *J. Biophysic. and Biochem. Cytol.*, 1961, **9**, 409.
17. REYNOLDS, E. S., The use of lead citrate at high pH as an electron-opaque stain in electron microscopy, *J. Cell Biol.*, 1963, **17**, 208.
18. BLOOM, W., and FAWCETT, D. W., A Textbook of Histology, 1962, Philadelphia, W. B. Saunders Co.
19. BOYD, W., Surgical Pathology, 1947, Philadelphia, W. B. Saunders Co.
20. FARQUHAR, M. G., and PALADE, G. E., Junctional complexes in various epithelia, *J. Cell Biol.*, 1963, **17**, 375.
21. CURRAN, P. F., Na, Cl and water transport by rat ileum *in vitro*, *J. Gen. Physiol.*, 1960, **43**, 1137.
22. CURRAN, P. F., and MCINTOSH, J. R., A model system for biological water transport, *Nature (London)*, 1962, **193**, 347.
23. OGILVIE, J. T., MCINTOSH, J. R., and CURRAN, P. F., Volume flow in a series-membrane system, *Biochim. et Biophysica Acta*, 1963, **66**, 441.
24. PATLAK, C. S., GOLDSTEIN, D. A., and HOFFMAN, J. F., The flow of solute and solvent across a two-membrane system, *J. Theoret. Biol.*, 1963, **5**, 426.
25. KAYE, G. I., and LANE, N., The epithelial basal complex: a morphophysiological unit in transport and absorption, *J. Cell Biol.*, 1965, **27**, 50A.
26. FARQUHAR, M. G., and PALADE, G. E., Functional organization of the amphibian skin, *Proc. Nat. Acad. Sc.*, 1964, **51**, 569.
27. OTERO-VILARDEBÓ, L. R., LANE, N., and GODMAN, G. C., Localization of phosphatase activities in colonic goblet and absorptive cells, *J. Cell Biol.*, 1964, **21**, 486.
28. BARTOSZEWICZ, W., and BARRNETT, R. J., Fine structural localization of nucleoside phosphatase activity in the urinary bladder of the toad, *J. Ultrastruct. Research*, 1964, **10**, 599.
29. KAYE, G. I., and TICE, L. W., Studies on the cornea. V. Electron microscopic localization of adenosinetriphosphatase activity in the rabbit cornea in relation to transport, *Inv. Ophth.*, 1966, **5**, 22.
30. WACHSTEIN, M., and BESEN, M., Electron microscopic study in several mammalian species of the reaction product enzymatically liberated from adenosinetriphosphate in the kidney, *Lab. Invest.*, 1964, **13**, 476.
31. GOLDFISCHER, S., ESSNER, E., and NOVIKOFF, A. B., The localization of phosphatase activity at the level of ultrastructure, *J. Histochem. and Cytochem.*, 1964, **12**, 72.
32. KAYE, G. I., and PAPPAS, G. D., Studies on the ciliary epithelium and zonule. III. The fine structure of the rabbit ciliary epithelium in relation to the localization of ATPase activity, *J. Micr.*, 1965, **4**, 497.
33. PEASE, D. C., Infolded basal membranes found in epithelia noted for their water transport, *J. Biophysic. and Biochem. Cytol.*, 1956, **2**, No. 4, suppl., 203.
34. MAXWELL, D. S., and PEASE, D. C., The electron microscopy of the choroid plexus, *J. Biophysic. and Biochem. Cytol.*, 1956, **2**, 467.
35. HOLMBERG, A., Ultrastructure of the ciliary epithelium, *Arch. Ophth.*, 1959, **62**, 935.
36. RHODIN, J., Correlation of ultrastructural organization and function in normal and experimentally changed proximal convoluted tubule cells of the mouse kidney, Karolinska Institutet, Stockholm, Aktiebolaget Godvil, 1954.
37. PAPPAS, G. D., and SMELSER, G. K., Studies on the ciliary epithelium and the zonule. I. Electron microscope observations on changes induced by alteration of normal aqueous humor formation in the rabbit, *Am. J. Ophth.*, 1958, **46**, (11) 299.
38. PAPPAS, G. D., SMELSER, G. K., and BRANDT, P. W., Studies on the ciliary epithelium and the zonule. II. Electron and fluorescence microscope observations on the function of membrane elaborations, *Arch. Ophth.*, 1959, **62**, 959; 1057.
39. PALAY, S. L., and KARLIN, L. J., An electron microscopic study of the intestinal villus. I. The fasting animal, *J. Biophysic. and Biochem. Cytol.*, 1959, **5**, 363.
40. PALAY, S. L., and KARLIN, L. J., An electron microscopic study of the intestinal villus. II. The pathway of fat absorption, *J. Biophysic. and Biochem. Cytol.*, 1959, **5**, 373.
41. LADMAN, A. J., PADYKULA, H. A., and STRAUSS, E. W., A morphological study of fat transport in the normal human jejunum, *Am. J. Anat.*, 1963, **112**, 389.

42. WISSIG, S. L., An electron microscope study of permeability of capillaries in muscle, *Anat. Rec.*, 1958, **130,** 467.
43. HAMPTON, J. C., An electron microscope study of the hepatic uptake and excretion of submicroscopic particles injected into the blood stream and into the bile duct, *Acta Anat.*, 1958, **32,** 262.
44. HAYWARD, A. F., Electron microscopic observations on absorption in the epithelium of the guinea pig gall bladder, *Z. Zellforsch.*, 1962, **56,** 197.
45. GRIM, E., A mechanism for absorption of sodium chloride solutions from the canine gall bladder, *Am. J. Physiol.*, 1963, **205,** 247.
46. KAYE, G. I., and PAPPAS, G. D., Studies on the cornea. I. The fine structure of the rabbit cornea and the uptake and transport of colloidal particles by the cornea *in vivo*, *J. Cell Biol.*, 1962, **12,** 457.
47. KAYE, G. I., PAPPAS, G. D., DONN, A., and MALLETT, N. M., Studies on the cornea. II. The uptake and transport of colloidal particles by the living rabbit cornea *in vitro*, *J. Cell Biol.*, 1962, **12,** 481.
48. KAYE, G. I., Studies on the cornea. III. The fine structure of the frog cornea and the uptake and transport of colloidal particles by the cornea *in vivo*, *J. Cell Biol.*, 1962, **15,** 241.
49. KAYE, G. I., and DONN, A., Studies on the cornea. IV. Some effects of ouabain on pinocytosis and stromal thickness in the rabbit cornea, *Inv. Ophth.*, 1965, **4,** 844.
50. KAYE, G. I., COLE, J. D., and DONN, A., Electron microscopy: Sodium localization in normal and ouabain-treated transporting cells, *Science*, 1965, **150,** 1167.
51. SABOUR, M. S., MACDONALD, M. K., LAMBIE, A. T., and ROBSON, J. S., The electron microscopic appearance of the kidney in hydrated and dehydrated rats, *Quart. J. Exp. Physiol.*, 1964, **49,** 162.
52. PHELPS, P. C., RUBIN, C. E., and LUFT, J. H., Electron microscope techniques for studying absorption of fat in man with some observations on pinocytosis, *Gastroenterology*, 1964, **46,** 134.
53. TRIER, J. S., PHELPS, P. C., and RUBIN, C. E., Electron microscopy of mucosa of small intestine, *J. Am. Med. Assn.*, 1963, **183,** 768.
54. TRIER, J. S., and RUBIN, C. E., Electron microscopy of the small intestine: a review, *Gastroenterology*, 1965, **49,** 574.
55. WERNER, H. J., and LUEBBEN, G. E., Electron nicroscopic observations of the epithelium of the intestinal tract of *Amphiuma means*, *Proc. Louisiana Acad. Sc.*, 1963, **26,** 84.
56. LASCHI, R., and GASBARRINI, G., Contributo allo studio dell'assorbimento intestinale mediante la microscopia elettronica, *Sperimentale*, 1963, **113,** 239.
57. ZETTERQUIST, H., The ultrastructural organization of the columnar absorbing cells of the mouse jejunum, Karolinska Institutet, Stockholm, Aktiebolaget Godvil, 1956.
58. IMAI, H., SAITO, S., STEIN, A. A., Ultrastructure of adenomatous polyps and villous adenomas of the large intestine, *Gastroenterology*, 1965, **48,** 188.
59. HAYWARD, A. F., and JOHNSTON, H. S., The fine structure of the epithelium of the colon in the mouse, *Scot. Med. J.*, 1961, **6,** 416.
60. CARASSO, N., FAVARD, P., and VALERIEN, J., Variations des ultrastructures dans les cellules épithéliales de la vessie du crapaud après stimulation par l'hormone neurohypophysaire, *J. Micr.*, 1962, **1,** 143.
61. PAK POY, R. K. F., and BENTLEY, P. J., Fine structure of the epithelial cells of the toad urinary bladder, *Exp. Cell Research*, 1960, **20,** 235.